www.newsteelconstruction.com

NSC TECHNICAL DIGEST 2018

Supplement to Volume 26

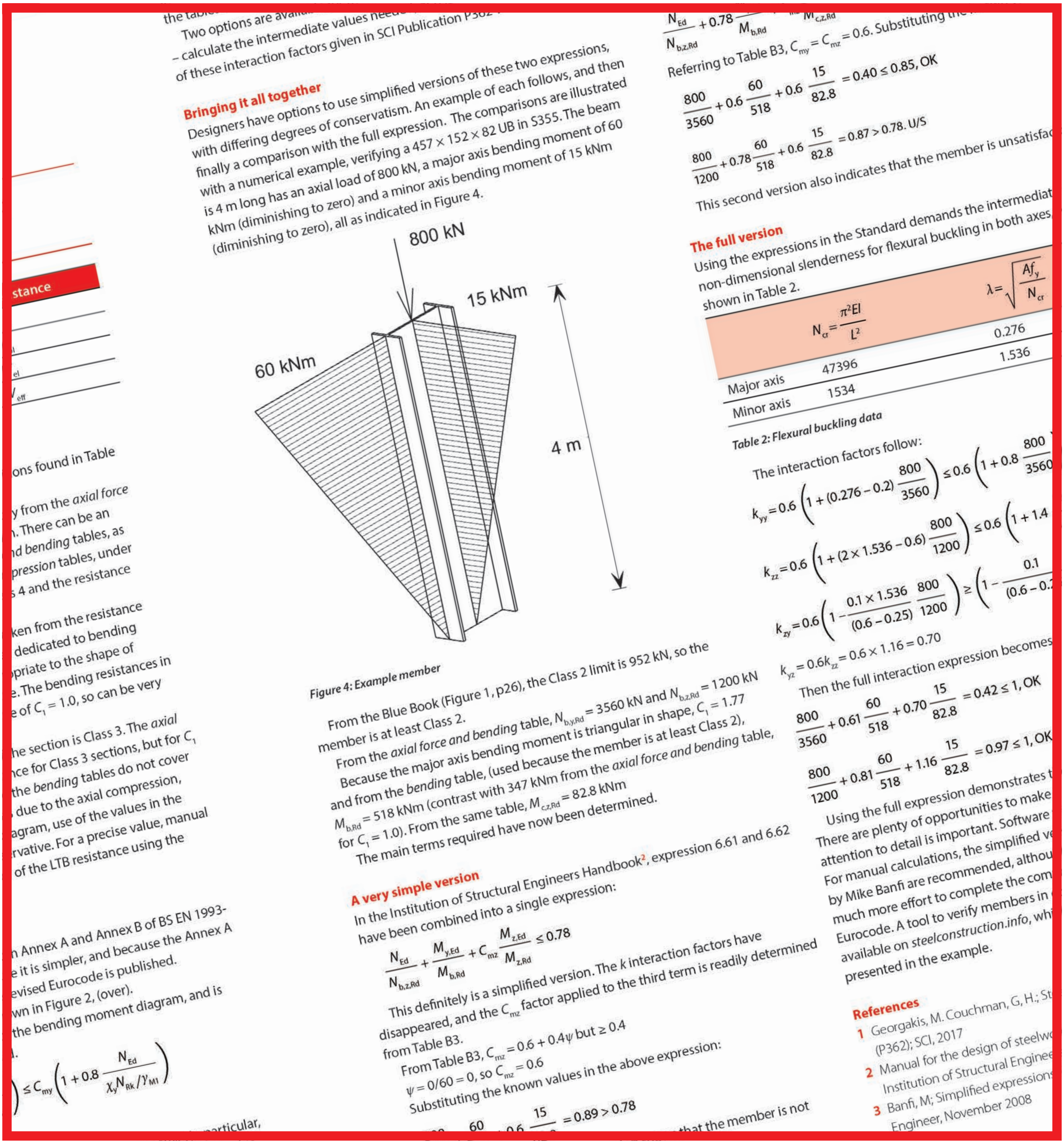
– calculate the intermediate values need... of these interaction factors given in SCI Publication P362...

Bringing it all together

Designers have options to use simplified versions of these two expressions, with differing degrees of conservatism. An example of each follows, and then finally a comparison with the full expression. The comparisons are illustrated with a numerical example, verifying a 457 × 152 × 82 UB in S355. The beam is 4 m long has an axial load of 800 kN, a major axis bending moment of 60 kNm (diminishing to zero) and a minor axis bending moment of 15 kNm (diminishing to zero), all as indicated in Figure 4.

Figure 4: Example member

From the Blue Book (Figure 1, p26), the Class 2 limit is 952 kN, so the member is at least Class 2.

From the *axial force and bending* table, $N_{b,y,Rd} = 3560$ kN and $N_{b,z,Rd} = 1200$ kN

Because the major axis bending moment is triangular in shape, $C_1 = 1.77$ and from the *bending* table, (used because the member is at least Class 2), $M_{b,Rd} = 518$ kNm (contrast with 347 kNm from the *axial force and bending* table, for $C_1 = 1.0$). From the same table, $M_{cz,Rd} = 82.8$ kNm

The main terms required have now been determined.

A very simple version

In the Institution of Structural Engineers Handbook[2], expression 6.61 and 6.62 have been combined into a single expression:

$$\frac{N_{Ed}}{N_{b,z,Rd}} + \frac{M_{y,Ed}}{M_{b,Rd}} + C_{mz}\frac{M_{z,Ed}}{M_{z,Rd}} \le 0.78$$

This definitely is a simplified version. The *k* interaction factors have disappeared, and the C_{mz} factor applied to the third term is readily determined from Table B3.

From Table B3, $C_{mz} = 0.6 + 0.4\psi$ but ≥ 0.4

$\psi = 0/60 = 0$, so $C_{mz} = 0.6$

Substituting the known values in the above expression:

... $= 0.89 > 0.78$

...that the member is not

Referring to Table B3, $C_{my} = C_{mz} = 0.6$. Substituting the...

$$\frac{800}{3560} + 0.6\frac{60}{518} + 0.6\frac{15}{82.8} = 0.40 \le 0.85, \text{OK}$$

$$\frac{800}{1200} + 0.78\frac{60}{518} + 0.6\frac{15}{82.8} = 0.87 > 0.78. \text{U/S}$$

This second version also indicates that the member is unsatisfac...

The full version

Using the expressions in the Standard demands the intermediat... non-dimensional slenderness for flexural buckling in both axes... shown in Table 2.

	$N_{cr} = \frac{\pi^2 EI}{L^2}$	$\lambda = \sqrt{\frac{Af_y}{N_{cr}}}$
Major axis	47396	0.276
Minor axis	1534	1.536

Table 2: Flexural buckling data

The interaction factors follow:

$$k_{yy} = 0.6\left(1 + (0.276 - 0.2)\frac{800}{3560}\right) \le 0.6\left(1 + 0.8\frac{800}{3560}\right.$$

$$k_{zz} = 0.6\left(1 + (2 \times 1.536 - 0.6)\frac{800}{1200}\right) \le 0.6\left(1 + 1.4\right.$$

$$k_{zy} = 0.6\left(1 - \frac{0.1 \times 1.536}{(0.6 - 0.25)}\frac{800}{1200}\right) \ge \left(1 - \frac{0.1}{(0.6 - 0.2}\right.$$

$k_{yz} = 0.6k_{zz} = 0.6 \times 1.16 = 0.70$

Then the full interaction expression becomes

$$\frac{800}{3560} + 0.61\frac{60}{518} + 0.70\frac{15}{82.8} = 0.42 \le 1, \text{OK}$$

$$\frac{800}{1200} + 0.81\frac{60}{518} + 1.16\frac{15}{82.8} = 0.97 \le 1, \text{OK}$$

Using the full expression demonstrates t... There are plenty of opportunities to make... attention to detail is important. Software... For manual calculations, the simplified ve... by Mike Banfi are recommended, althou... much more effort to complete the com... Eurocode. A tool to verify members in ... available on *steelconstruction.info*, whi... presented in the example.

References

1 Georgakis, M. Couchman, G. H.; St... (P362); SCI, 2017
2 Manual for the design of steelw... Institution of Structural Enginee...
3 Banfi, M; Simplified expressions... Engineer, November 2008

NSC

Technical Digest
2018

EDITOR
Nick Barrett Tel: 01323 422483
nick@newsteelconstruction.com

DEPUTY EDITOR
Martin Cooper Tel: 01892 538191
martin@newsteelconstruction.com

PRODUCTION EDITOR
Andrew Pilcher Tel: 01892 553147
admin@newsteelconstruction.com

PRODUCTION ASSISTANT
Alastair Lloyd Tel: 01892 553145
alastair@barrett-byrd.com

COMMERCIAL MANAGER
Fawad Minhas Tel: 01892 553149
fawad@newsteelconstruction.com

NSC IS PRODUCED BY BARRETT BYRD ASSOCIATES ON BEHALF OF THE BRITISH CONSTRUCTIONAL STEELWORK ASSOCIATION AND STEEL FOR LIFE IN ASSOCIATION WITH THE STEEL CONSTRUCTION INSTITUTE

The British Constructional Steelwork Association Ltd
4 Whitehall Court, Westminster, London SW1A 2ES
Telephone 020 7839 8566
Website *www.steelconstruction.org*
Email *postroom@steelconstruction.org*

Steel for Life Ltd
4 Whitehall Court, Westminster, London SW1A 2ES
Telephone 020 7839 8566
Website *www.steelforlife.org*
Email *steelforlife@steelconstruction.org*

The Steel Construction Institute
Silwood Park, Ascot, Berkshire SL5 7QN
Telephone 01344 636525 Fax 01344 636570
Website *www.steel-sci.com*
Email *reception@steel-sci.com*

CONTRACT PUBLISHER & ADVERTISING SALES
Barrett, Byrd Associates
7 Linden Close,
Tunbridge Wells, Kent TN4 8HH
Telephone 01892 524455
Website *www.barrett-byrd.com*

These and other steelwork articles can be downloaded from the New Steel Construction Website at *www.newsteelconstruction.com*

Keeping designers up-to-date

Nick Barrett - Editor

The steel construction sector's annual series of Technical Digests has proven to be a popular addition to the flow of information for architects and engineers since its launch two years ago.

This is the third in the series of digests, and along with the previous two is always available for download at the steelconstruction.info website.

The steel construction sector has a long-established reputation for doing everything that can be done to keep designers in steel up-to-date with all the technical guidance needed to ensure that they can take advantage of the numerous benefits of steel as a construction material. A comprehensive array of ways of accessing this information ensures that guidance and information is never more than a couple of clicks away. Everything relevant to steel construction including cost as well as design guidance, is freely available on the steelconstruction.info website, the free to use first port of call for technical support.

The BCSA's monthly magazine New Steel Construction (NSC) is another popular source of advice, including the highly popular Advisory Desk Notes and longer Technical Articles from the steel sector's own experts.

This Digest brings all the Advisory Desk Notes and Technical Articles published in NSC in 2018 together in a format that is available as downloadable pdfs or for online viewing.

AD Notes keep designers abreast of developments in technical standards. Some of them are provided following questions being asked of the sector's technical advisers. They are acknowledged as essential reading for all involved in the design of constructional steelwork.

The more detailed Technical Articles offer deeper insights into what designers need to know to produce the best steel construction projects. These articles can be initiated by legislative changes or changes to codes and standards.

Occasionally a technical update will be provided when it is felt that it would be useful if a lot of relatively minor changes were brought together in one place.

Both AD Notes and Technical Articles can provide early warnings to designers of changes that they need to know about and point towards sources of further detailed information available via the steel sector's other advisory routes. We hope you will continue to find this new publication of value.

Stainless steel in construction

Stainless steels may appear to be more suitable for teaspoons and kitchen sinks than for structural elements, but they can be used for support and other structures in aggressive environments, says Nancy Baddoo of SCI.

The main property that distinguishes stainless steel from carbon steel is that it possesses inherent corrosion resistance, due to the tightly adherent protective layer of chromium oxide which spontaneously forms on its surface in the presence of oxygen. This means that stainless steel components can be exposed to a wide range of environments without the need for protective coatings.

Stainless steels are highly versatile materials, possessing a unique selection of useful properties which can be exploited in load-bearing applications where cost is not a primary consideration. Figures 1 and 2 show stress-strain characteristics at low and high strains, compared against carbon steel. Austenitic stainless steels are generally used for structural applications, though the use of duplex stainless steel is increasing, where the higher strength is beneficial. The distinctive mechanical properties - considerable strain-hardening and ductility - make austenitic and duplex stainless steel particulalry well suited for structures required to withstand accidental loading.

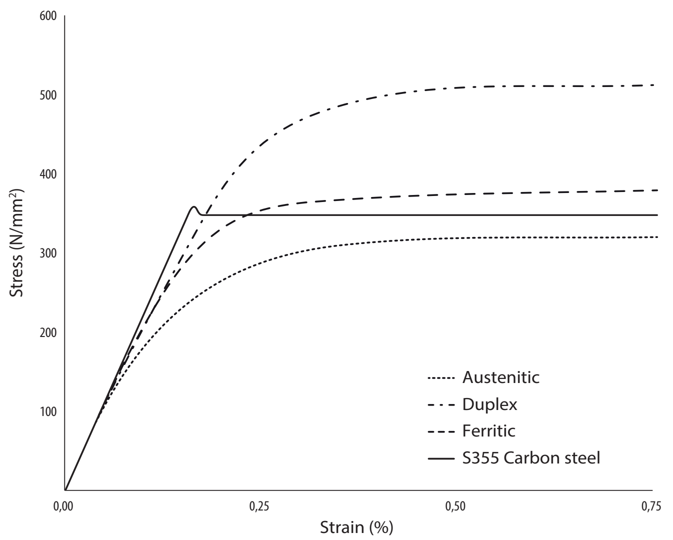

Figure 1 Stress-strain curves for stainless steel and carbon steel from 0 to 0.75 % strain

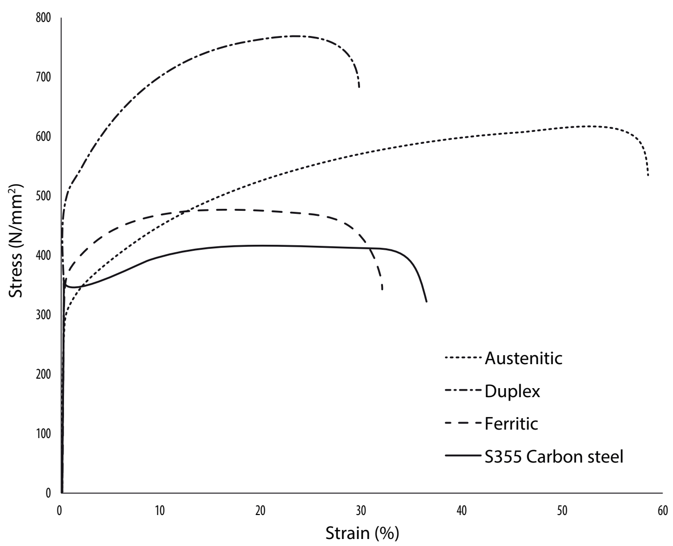

Figure 2 Full range stress-strain curves for stainless steel and carbon steel

Typical load-bearing applications include:

- Platforms and supports in processing plant for the water treatment, pulp and paper, nuclear, biomass, chemical, pharmaceutical, and food and beverage industries where the aggressive environment requires it.
- Pins, barriers, railings, cable sheathing and expansion joints in bridges
- Seawalls, piers and other coastal structures
- Reinforcing bar in concrete structures
- Curtain walling, roofing, canopies, tunnel lining
- Support systems for curtain walling, masonry, tunnel lining etc
- Security barriers, hand railing, street furniture
- Fasteners and anchoring systems in wood, stone, masonry or rock
- Structural members and fasteners in swimming pool buildings (special precautions should be taken for structural components in swimming pool atmospheres due to the risk of stress corrosion cracking in areas where condensates may form).
- Explosion- and impact- resistant structures such as security walls, gates and bollards
- Fire and explosion resistant walls, cable ladders and walkways on offshore platforms

In 2017, a new 160 m footbridge was constructed adjacent to the Grade 2 listed Countess Wear Bridge (figures 3 & 4) in order to create a 3 m wide pedestrian and cycle route. The new footbridge comprises nine spans using conventional carbon steel and is supported in part by five hidden cantilevers embedded into the piers of the stone bridge, made from 1.4462 (2205) duplex stainless steel box sections.

The use of cantilevers avoided the need for work to be carried out in the river and complemented the appearance of the historic bridge rather than obscuring it. For these structurally critical components stainless steel was chosen for strength (grade 1.4462 stainless steel has a design strength of 450 MPa), to meet the 120 year design life target and because they were difficult to inspect and maintain.

The cantilevers are supported by piles carrying tension forces through the stone bridge into the bedrock 20 m below by means of stainless steel threaded bars. The parapet posts and handrails along the bridge were also made from duplex stainless steel. The client and designer for the project was Devon County Council and the steelwork was fabricated and installed by Taziker Industrial.

Although sharing many similar mechanical properties with carbon steel, the non-linear stress-strain characteristics mean that different design rules are needed for stainless steel. The non-linearity primarily affects local and global buckling response with some section classification limits being stricter.

Design standards for stainless steel have developed around the world. In Europe, when Eurocode 3: Part 1.4 was published in 2006 [1], it was the first design standard for stainless steel in almost all European countries and the only design standard in the world which covered hot rolled, welded and cold formed products, as well as design in the fire situation. EN 1993-1-4 is a brief standard, just giving supplementary rules where the rules for carbon steel given in EN 1993-1-1 [2], EN 1993-1-3 [3], EN 1993-1-5 [4] and EN 1993-1-8 [5] are not applicable.

In certain places the rules in the 2006 edition of EN 1993-1-4 were very conservative with limited scope due to a shortage of test data. However, over the last 10 years or so there has been a very significant increase in research into the structural performance of stainless steel in Europe and worldwide and much useful information has been generated. The international database of

Figures 3 & 4: Countess Wear Footbridge: Left: Stainless steel cantilevers being lifted into position during a night closure; Right: Stainless steel parapet posts and handrails

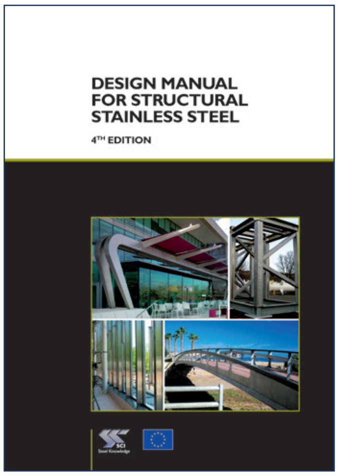

Figure 5: Design Manual for Structural Stainless Steel, Fourth Edition, 2017

structural tests is now three times larger than what was used to derive the original stainless steel Eurocode rules. As a result of the availability of these new research data, it was possible to develop improvements to the rules in the 2006 edition of EN 1993-1-4 and an amendment to the rules was published in 2015. The new rules permit less conservative design and extend the range of grades to which the rules apply (the grades listed in the standard did not reflect current usage). Efficient design methods are essential for stainless steel because of its high cost relative to carbon steel.

The most significant revision to the structural design rules in the 2015 amendment concern section classification: the limiting width to thickness ratios have been increased to align with those for carbon steel, except for internal compression elements. Additionally, less conservative shear buckling guidance has been included and clearer guidance on how to design cold worked stainless steel.

A key difference between stainless steel and carbon steel is that there are a wide range of stainless steel grades, each with slightly different compositions and hence corrosion resistance. Another significant revision in the 2015 amendment of EN 1993-1-4 was the inclusion of a step-by-step procedure for grade selection. The procedure involves the following steps:

- Determination of the **Corrosion Resistance Factor (CRF)** for the environment
- Determination of the **Corrosion Resistance Class (CRC)** from the CRF

The CRF depends on the severity of the environment and is calculated as follows:

$$\mathrm{CRF} = F_1 + F_2 + F_3$$

where

F_1 = Risk of exposure to chlorides from salt water or de-icing salts;

F_2 = Risk of exposure to sulphur dioxide;

F_3 = Cleaning regime or exposure to washing by rain.

The CRF considers all corrosion risks including pitting, crevice corrosion and stress corrosion cracking of stainless steels that may affect integrity of load bearing parts. The assumption in the selection procedure is that no corrosion of stainless steel will occur that would impact the structural integrity of a load-bearing component. However, in some instances cosmetic corrosion (staining or minor pitting) could occur. These effects may be unsightly and unacceptable where appearance is important but are not detrimental to integrity.

Grades of stainless steel are classified in one of five CRCs, with CRC V being the most durable (e.g. containing grades suitable for the highly corrosive atmospheres above indoor swimming pools). The final choice of a specific grade within a CRC will depend on other factors in addition to corrosion resistance, such as strength and availability in the required product form. It is sufficient for the designer to specify the material by CRC and design strength, e.g. CRC II and $f_y = 450\ \mathrm{N/mm^2}$.

The publication of the amendment rendered all existing resources for designers relating to the stainless Eurocode obsolete. A new collection of supporting design resources is being prepared in order to help designers to use the new rules in the European dissemination project PUREST (Promotion of new Eurocode rules for structural stainless steel), part funded by the EU's Research Fund for Coal and Steel. The 18 month project started in 2016 and finished in December 2017 and involved partners from Germany, Belgium, Spain, Portugal, Czech Republic, Finland, Sweden, Poland and Italy. SCI co-ordinated the work with support from Imperial College London and Arup.

Activities were mostly targeted at design practitioners and included:

- Updating and extending the *Design Manual for Structural Stainless Steel*,
- Translating the *Design Manual* from English into 9 languages,
- Developing online design software and design apps,
- National seminars and recording webinars for distance learning.

SCI published the Fourth Edition of the *Design Manual for Structural Stainless Steel* in 2017[6] (Figure 5). It consists of three parts:

- **Recommendations**, which give the design guidance and essential information needed by designers concerning grade selection, durability, material properties, design rules and fabrication
- **Commentary**, which explains how the design expressions in the Recommendations were derived and gives background information and references
- **Design Examples**, which demonstrate the use of the Recommendations

As well as updating the design rules to align with the 2015 amendment to EN 1993-1-4, the *Design Manual* also includes information on ferritic stainless steels. These grades are generally used in gauges of 4 mm and below, and offer a corrosion resistant alternative to many light gauge galvanized steel applications.

Additionally two new design methods are included. The first gives rules on how to take advantage of the work hardening associated with cold forming operations during fabrication (a strength enhancement of about 50 % is typical in the cold formed corners of cross sections, and the strength of the material in the flat faces also increases). The second gives a method for calculating the enhanced cross-section design resistances due to the beneficial influence of work hardening in service using the Continuous Strength Method.

All the design resources developed in the PUREST project are accessible at www.steel-stainless.org/designmanual.

For more information, please contact Nancy Baddoo at SCI (n.baddoo@steel-sci.com).

References:

1 EN 1993-1-4:2006+A1:2015 Eurocode 3. Design of steel structures. General rules. Supplementary rules for stainless steels
2 EN 1993-1-1:2005+A1:2014 Eurocode 3. Design of steel structures. General rules and rules for buildings
3 EN 1993-1-3:2006 Eurocode 3. Design of steel structures. General rules. Supplementary rules for cold-formed members and sheeting
4 EN 1993-1-5:2006 Eurocode 3. Design of steel structures. Plated structural elements
5 EN 1993-1-8:2005 Eurocode 3. Design of steel structures. Design of joints
6 Design Manual for Structural Stainless Steel, SCI Publication P413, 2017

Cold formed sections

The forming process affects the toughness of cold formed sections and their use in external structures. Welding is prohibited near the corners of cold formed sections in certain circumstances. Richard Henderson of the SCI discusses the issues.

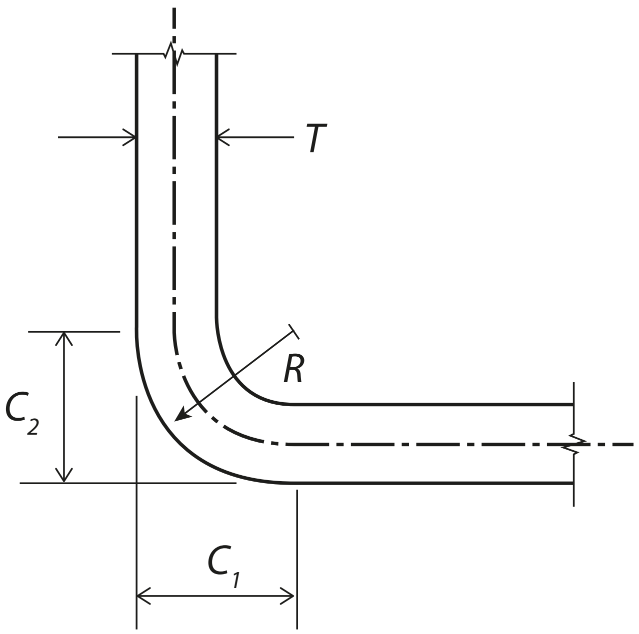

Figure 1: Corner dimensions

The toughness of steel is affected by the extent of strain it has undergone as well as by other factors. This fact is taken into account when determining the limiting thickness for materials using BS EN 1993-1-10. The limiting thickness of plate or hot rolled or hot finished structural sections does not, in general, depend on the extent of strain because such elements are not subject to plastic strain during their use, nor in the course of their manufacture. This does not apply however to cold formed square and rectangular hollow sections, which experience significant strains at the corners of the profile. Neither does it apply to beams which have been pre-cambered by cold bending.

The product standard for cold formed welded structural hollow sections, BS EN 10219-1:2006 requires that for square or rectangular sections, the test pieces for impact testing are taken either longitudinally or transversely midway between the corners from one of the sides not containing the weld. The impact values therefore relate to material which is unaffected by cold forming, thus tacitly acknowledging that the forming process affects the material toughness. According to clause 6.7.2 of the product standard, there is no requirement for impact tests for specified thicknesses of less than 6 mm.

The effect of strain during cold forming must be taken into account when determining the limiting thickness of material of a given sub-grade. According to BS EN 1993-1-10 and its UK National Annex, the reference temperature T_{Ed} for determining the toughness of a steel element:

$$T_{Ed} = T_{md} + \Delta T_r + \Delta T_\sigma + \Delta T_R + \Delta T_\varepsilon + \Delta T_{\varepsilon cf}$$

where (T_{md}+ΔT_r) considered together represent the minimum effective temperature of the steel part, ΔT_R is a safety allowance, ΔT_ε is an adjustment for strain rate and $\Delta T_{\varepsilon cf}$ is an adjustment for the extent of strain during cold forming.

The UK National Annex collects together factors affecting the safety of elements and gives an equation for ΔT_R as follows:

$$\Delta T_R = \Delta T_{RD} + \Delta T_{Rg} + \Delta T_{RT} + \Delta T_{R\sigma} + \Delta T_{Rs}$$

where ΔT_{RD} is an adjustment for detail type, ΔT_{Rg} for gross stress concentration, ΔT_{RT} for Charpy test temperature, $\Delta T_{R\sigma}$ for stress level and ΔT_{Rs} for strength grade. The procedure is consistent with $\Delta T_\sigma = 0$.

The temperature adjustment for cold forming is given in clause 2.3.1(2) of the standard as minus three times the percentage strain expressed as degrees Celsius. A strain of 10% would result in a temperature adjustment of −30 °C. This is potentially significant when considering the adoption of cold formed sections.

The strain resulting from cold forming SHS or RHS tubes can be determined from the limiting dimensions in the product standard as follows. Consider the corner of a box section as shown in Figure 1. The external corner profile is determined in the product standard by measuring dimensions C_1 and C_2 or R.

The length of the centre line is the original length before forming. For one corner, the centre line length is:

$$L = \frac{2\pi}{4}\left(R - \frac{T}{2}\right)$$

The outside length after forming is $\frac{2\pi}{4}R$

The change in length $\Delta L = \frac{2\pi}{4}R - \frac{2\pi}{4}\left(R - \frac{T}{2}\right) = \frac{\pi T}{4}$

The strain is $\frac{\pi T/4}{2\pi/4(R-T/2)} = \frac{T}{(2R-T)}$

The dimensional tolerances on the corner radius for different thickness ranges is taken from the product standard and used to determine the maximum percent strain due to cold forming in Table 1 by substituting the minimum external radius in the formula for strain.

Thickness Range (mm)	External corner profile C_1 and C_2 or R	Maximum strain	% strain
$0 < t \le 6$	1.6*T* to 2.4*T*	$T/(2\times1.6T - T) = 1/2.2$	45.5
$6 < t \le 10$	2.0*T* to 3.0*T*	$T/(2\times2.0T - T) = 1/3.0$	33.3
$10 < t$	2.4*T* to 3.6*T*	$T/(2\times2.4T - T) = 1/3.8$	26.3

Table 1: Strain due to cold forming

The strain could therefore be as high as 45% for material less than 6 mm thick bent to the tightest radius, giving a temperature adjustment for cold forming of -3 × 45 = −135 °C when determining the limiting thickness. Such an adjustment puts the relevant temperature well outside the range covered by the tables in BS EN 1993-1-10 and PD 6695-1-10.

The SCI's recent publication P419, Brittle fracture: selection of steel subgrade to BS EN 1993-1-10 addresses the acknowledged conservatism in the standard for structures where fatigue is not a significant design consideration and presents tables of limiting material thicknesses for this circumstance. However, the tables do not extend to the much lower temperatures indicated when considering the adjustments for the high strains resulting from cold forming. SCI has produced values for the relevant temperatures and these are given in Table 2 for S355J2 material (the common steel grade for hollow sections).

Material S355J2	Stress level $0.75f_y$											
Temperature (°C)	-70	-80	-90	-100	-110	-120	-130	-140	-150	-160	-170	-180
Thickness (mm)	54	40	30	32	18	15	12	10	8	7	6	5

Table 2: Limiting thicknesses for low temperatures

Adjustment	$(T_{md} + \Delta T_r)$	ΔT_{RD}	ΔT_{Rg}	ΔT_{RT}	$\Delta T_{R\sigma}$	ΔT_{RS}	ΔT_{ε}	$\Delta T_{\varepsilon cf}$	Total
Temperature (°C)	-15	-30	0	0	0	0	0	-136	-181

Table 3: Temperature adjustments for determining limiting thickness

As an example consider a cold formed section of steel grade S355J2 with thickness in the range 0 to 6 mm used in an external building environment where fatigue is not a design consideration, with a high design stress ($\sigma_{Ed} > 0.5f_y$), no gross stress concentration and with a welded detail classed as "Welded very severe".

Temperature adjustments are given in Table 3.

From Table 2, the limiting thickness of the cold formed section is 5 mm. Limiting thicknesses for sections in the higher thickness ranges in the product standard are given in Tables 4 and 5 for details classed as "welded very severe" and "welded severe".

Table 5 also applies to a detail which is classed as "welded very severe" and has a design stress of less than $0.3f_y$.

An examination of the sizes in the Blue Book shows that certain sections should not be used if the attributes of a connection detail correspond to those in Table 4. If the detail corresponds to the description in Table 5, there is no restriction on the catalogue sizes which could be used.

The strain involved in cold forming circular hollow sections is much less than that at the corners of square and rectangular sections (about 10% in the worst case) and there is consequently no restriction on the choice of cold formed circular hollow sections, even with the presence of a gross stress concentration.

Designers will also remember that BS EN 1993-1-8:2005 Clause 4.14 and Table 4.2 imposes restrictions on welding near cold formed zones. The table is entitled 'Conditions for welding cold formed zones and adjacent material' and gives maximum thicknesses based on an *r/t* ratio or strain due to cold forming. Unhelpfully, the radius considered in the clause is the internal radius of the corner, whereas the product standard BS EN 10219-2 uses the external radius (external corner profile). The corresponding *r/t* values and limiting thicknesses are given in Table 6 (right).

The clause therefore prohibits welding within 5 times the wall thickness of the corners of many square and rectangular cold formed sections, unless the steel is "fully killed Aluminium-killed steel (Al ≥ 0.02%)", with limits on carbon (C ≤ 0.18%,), phosphorous (P ≤ 0.02%) and sulphur (S ≤ 0.012%). Alternatively, tests must have been carried out to show that welding is permitted.

Table A1 in Annex A of the product standard indicates the steel is fully killed steel with a minimum 0.02% of total aluminium. The table gives the chemical composition of the steel and includes maximum percentages by mass of carbon (C ≤ 0.22%), phosphorous (P ≤ 0.03%) and sulphur (S ≤ 0.03%). The material therefore satisfies the requirement for fully-killed aluminium killed steel but allows the percentage of carbon, phosphorous and sulphur to fall outside the limits specified in Table 4.2.

This restriction prohibits the adoption of a welded end plate or base plate for most rectangular and square cold formed hollow sections which comply with the product standard but do not meet the tighter requirements for carbon, phosphorous and sulphur in Table 4.2.

Design detail	Thickness range (mm)	Temperature adjustment (°C)	Maximum thickness (mm)
no fatigue; external steelwork, welded very severe, high design stress (>$0.5f_y$) no gross stress concentration, S355J2H	$0 < t \leq 6$	-181	5
	$6 < t \leq 10$	-145	9
	$10 < t$	-124	13

Table 4: Detail classed as welded very severe (equivalent to -30 °C in NA.1)

Design detail	Thickness range (mm)	Temperature adjustment (°C)	Maximum thickness (mm)
no fatigue; external steelwork, welded severe, high design stress (>$0.5f_y$) no gross stress concentration, S355J2H	$0 < t \leq 6$	-171	6
	$6 < t \leq 10$	-135	11
	$10 < t$	-114	16

Table 5: Detail which is classed as welded severe (equivalent to -20 °C in NA.1)

Product standard thickness range (mm)	Product standard tolerances based on *R*	Table 4.2 Corresponding *r/t*	Table 4.2 "worst case" maximum thickness (mm)
$0 < t \leq 6$	$1.6T$ to $2.4T$	0.6 to 1.4	not given
$6 < t \leq 10$	$2.0T$ to $3.0T$	1.0 to 2.0	6
$10 < t$	$2.4T$ to $3.6T$	*1.4 to 2.6*	6 (out of range)

Table 6: Maximum thickness for welding related to the product standard

Members subject to combined bending and compression

David Brown of the SCI reviews the options and available resources that can be used to simplify the design checks and determine the required resistance data.

Expressions 6.61 and 6.62

These two expressions are well-known in the Eurocode steel design world. They bring together a number of intermediate calculations in a final crescendo of complexity, not helped by an unfamiliar presentation of familiar terms. In fact, the expressions are conceptually similar to the "more exact" approaches found in BS 5950, containing an axial term, a major axis moment term and a minor axis moment term. The denominators in the three terms are the flexural buckling resistance, the lateral torsional buckling resistance and the minor axis cross sectional resistances respectively. The second two terms are modified by factors that allow for the interaction between the different modes of buckling.

If Class 4 sections are excluded the ΔM terms due to a shift in the neutral axis can be removed, and if the denominators are presented in more familiar terms, the two expressions become:

$$\frac{N_{\mathrm{Ed}}}{N_{\mathrm{b,y,Rd}}} + k_{yy}\frac{M_{\mathrm{y,Ed}}}{M_{\mathrm{b,Rd}}} + k_{yz}\frac{M_{\mathrm{z,Ed}}}{M_{\mathrm{c,z,Rd}}} \leq 1 \quad (6.61)$$

$$\frac{N_{\mathrm{Ed}}}{N_{\mathrm{b,z,Rd}}} + k_{zy}\frac{M_{\mathrm{y,Ed}}}{M_{\mathrm{b,Rd}}} + k_{zz}\frac{M_{\mathrm{z,Ed}}}{M_{\mathrm{c,z,Rd}}} \leq 1 \quad (6.62)$$

The main ratios are each $\frac{\text{applied}}{\text{resistance}}$. Purists should note that the denominator in the final term is really $\frac{W_z f_y}{\gamma_{\mathrm{M1}}}$, but this is equal to the cross sectional resistance $M_{\mathrm{c,z,Rd}}$ since $\gamma_{\mathrm{M1}} = \gamma_{\mathrm{M0}} = 1.0$

The first task in using these expressions is to determine the member resistances.

Member resistances from the Blue Book

The calculation of member resistances always starts from section classification. The easy way to classify a section under combined bending and axial load is to use the "*n*" limit given in the *axial force and bending* tables of the Blue Book.

Section Designation and Axial Force Resistance $N_{\mathrm{pl,Rd}}$ (kN)	n Limit Class 3 **Class 2**
457x152x82 $N_{\mathrm{pl,Rd}}$ = 3620	0.839 **0.263**

Figure 1:"n" limit from the Blue Book

An extract from the tables is shown in Figure 1.

The Class 2 limit is the axial load ratio (compared to $N_{\mathrm{pl,Rd}}$) when a member changes from Class 2 to Class 3. The Class 3 limit is the axial load ratio when a section becomes Class 4 (and the designer may prefer to choose a different section!).

The limitations are so defined because, as shown in Table 1, the different Classes demand different properties to be used in the calculation of member resistance.

For the resistance calculations, it does not matter if the member is Class 1 or 2; both use the same member properties. Thus all that is needed is to know that the member is "at least Class 2", and hence why a Class 1 limit is not needed.

For the beam data shown in Figure 1, the member becomes Class 3 when the axial load exceeds 0.263 × 3620 = 952 kN. The member becomes Class 4 when the axial load exceeds 0.839 × 3620 = 3037 kN.

Class	Axial resistance	Bending resistance
1	A_g	W_{pl}
2	A_g	W_{pl}
3	A_g	W_{el}
4	A_{eff}	W_{eff}

Table 1: Member class and resistance calculations

These limits are simply a rearrangement of the conditions found in Table 5.2 of BS EN 1993-1-1.

Flexural buckling resistances can be obtained directly from the *axial force and bending* tables for the appropriate buckling length. There can be an advantage in taking resistances from the *axial force and bending* tables, as the resistances are limited to Class 3. In the pure *compression* tables, under uniform compression, the section may become Class 4 and the resistance penalised.

Lateral torsional buckling resistances are best taken from the resistance table for bending alone. This is because the tables dedicated to bending alone allow designers to select a resistance appropriate to the shape of bending moment diagram, based on the C_1 value. The bending resistances in the axial force and bending tables are for a value of C_1 = 1.0, so can be very conservative.

There is however an immediate problem if the section is Class 3. The *axial force and bending* tables provide a LTB resistance for Class 3 sections, but for C_1 = 1.0. All UB in bending alone are Class 1, so the *bending* tables do not cover Class 3 sections. If a section becomes Class 3 due to the axial compression, but has a non-uniform bending moment diagram, use of the values in the *axial force and bending* tables will be conservative. For a precise value, manual calculations would require the calculation of the LTB resistance using the elastic modulus.

The interaction factors

The interaction factors are given in both Annex A and Annex B of BS EN 1993-1-1. Annex B is recommended, because it is simpler, and because the Annex A method is to be relegated when the revised Eurocode is published.

A typical term from Annex B is shown in Figure 2, (below).

The *C* factor deals with the shape of the bending moment diagram, and is taken from Table B3 of the Standard.

$$k_{yy} = C_{my}\left(1 + (\bar{\lambda}_y - 0.2)\frac{N_{\mathrm{Ed}}}{\chi_y N_{\mathrm{Rk}}/\gamma_{\mathrm{M1}}}\right) \leq C_{my}\left(1 + 0.8\frac{N_{\mathrm{Ed}}}{\chi_y N_{\mathrm{Rk}}/\gamma_{\mathrm{M1}}}\right)$$

Figure 2: Typical interaction factor

Again, the presentation of these terms is not very attractive. In particular, the term $\chi_y N_{\mathrm{Rk}}/\gamma_{\mathrm{M1}}$ is unhelpful, as it is simply the flexural resistance (in this case in the major axis), or $N_{\mathrm{b,y,Rd}}$. The expressions might more helpfully be presented in the form in Figure 3.

$$k_{yy} = C_{my}\left(1 + (\bar{\lambda}_y - 0.2)\frac{N_{\mathrm{Ed}}}{N_{\mathrm{b,y,Rd}}}\right) \leq C_{my}\left(1 + 0.8\frac{N_{\mathrm{Ed}}}{N_{\mathrm{b,y,Rd}}}\right)$$

Figure 3: Typical interaction factor, revised presentation

The Blue Book cannot help here, as the expression demands an intermediate value, $\overline{\lambda}_y$ used as part of the calculation process, but not given in the tables.

Two options are available for the designer wanting to follow the full process – calculate the intermediate values needed, or use the graphical presentation of these interaction factors given in SCI Publication P362[1].

Bringing it all together

Designers have options to use simplified versions of these two expressions, with differing degrees of conservatism. An example of each follows, and then finally a comparison with the full expression. The comparisons are illustrated with a numerical example, verifying a 457 × 152 × 82 UB in S355. The beam is 4 m long has an axial load of 800 kN, a major axis bending moment of 60 kNm (diminishing to zero) and a minor axis bending moment of 15 kNm (diminishing to zero), all as indicated in Figure 4.

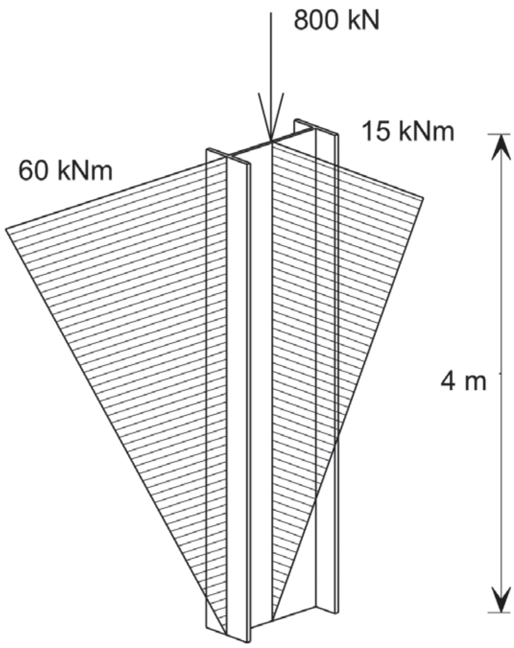

Figure 4: Example member

From the Blue Book (Figure 1, p8), the Class 2 limit is 952 kN, so the member is at least Class 2.

From the *axial force and bending* table, $N_{b,y,Rd} = 3560$ kN and $N_{b,z,Rd} = 1200$ kN

Because the major axis bending moment is triangular in shape, $C_1 = 1.77$ and from the *bending* table, (used because the member is at least Class 2), $M_{b,Rd} = 518$ kNm (contrast with 347 kNm from the *axial force and bending* table, for $C_1 = 1.0$). From the same table, $M_{c,z,Rd} = 82.8$ kNm

The main terms required have now been determined.

A very simple version

In the Institution of Structural Engineers Handbook[2], expression 6.61 and 6.62 have been combined into a single expression:

$$\frac{N_{Ed}}{N_{b,z,Rd}} + \frac{M_{y,Ed}}{M_{b,Rd}} + C_{mz}\frac{M_{z,Ed}}{M_{z,Rd}} \leq 0.78$$

This definitely is a simplified version. The *k* interaction factors have disappeared, and the C_{mz} factor applied to the third term is readily determined from Table B3.

From Table B3, $C_{mz} = 0.6 + 0.4\psi$ but ≥ 0.4

$\psi = 0/60 = 0$, so $C_{mz} = 0.6$

Substituting the known values in the above expression:

$$\frac{800}{1200} + \frac{60}{518} + 0.6\frac{15}{82.8} = 0.89 > 0.78$$

In this instance, the simple expression shows that the member is not satisfactory.

A *reasonably* simple version

Mike Banfi of Arup proposed a pair of simplified expressions in a technical note published in 2008[3]. For Class 1 or 2 sections, the simplified expressions are:

$$\frac{N_{Ed}}{N_{b,y,Rd}} + C_{my}\frac{M_{y,Ed}}{M_{b,Rd}} + C_{mz}\frac{M_{z,Ed}}{M_{c,z,Rd}} \leq 0.85 \text{ and}$$

$$\frac{N_{Ed}}{N_{b,z,Rd}} + 0.78\frac{M_{y,Ed}}{M_{b,Rd}} + C_{mz}\frac{M_{z,Ed}}{M_{c,z,Rd}} \leq 0.78$$

Referring to Table B3, $C_{my} = C_{mz} = 0.6$. Substituting the known values:

$$\frac{800}{3560} + 0.6\frac{60}{518} + 0.6\frac{15}{82.8} = 0.40 \leq 0.85, \text{ OK}$$

$$\frac{800}{1200} + 0.78\frac{60}{518} + 0.6\frac{15}{82.8} = 0.87 > 0.78. \text{ U/S}$$

This second version also indicates that the member is unsatisfactory.

The full version

Using the expressions in the Standard demands the intermediate values of non-dimensional slenderness for flexural buckling in both axes, which are shown in Table 2.

	$N_{cr} = \frac{\pi^2 EI}{L^2}$	$\overline{\lambda} = \sqrt{\frac{Af_y}{N_{cr}}}$
Major axis	47396	0.276
Minor axis	1534	1.536

Table 2: Flexural buckling data

The interaction factors follow:

$$k_{yy} = 0.6\left(1 + (0.276 - 0.2)\frac{800}{3560}\right) \leq 0.6\left(1 + 0.8\frac{800}{3560}\right) = 0.61$$

$$k_{zz} = 0.6\left(1 + (2 \times 1.536 - 0.6)\frac{800}{1200}\right) \leq 0.6\left(1 + 1.4\frac{800}{1200}\right) = 1.16$$

$$k_{zy} = 0.6\left(1 - \frac{0.1 \times 1.536}{(0.6 - 0.25)}\frac{800}{1200}\right) \geq \left(1 - \frac{0.1}{(0.6 - 0.25)}\frac{800}{1200}\right) = 0.81$$

$k_{yz} = 0.6k_{zz} = 0.6 \times 1.16 = 0.70$

Then the full interaction expression becomes

$$\frac{800}{3560} + 0.61\frac{60}{518} + 0.70\frac{15}{82.8} = 0.42 \leq 1, \text{ OK}$$

$$\frac{800}{1200} + 0.81\frac{60}{518} + 1.16\frac{15}{82.8} = 0.97 \leq 1, \text{ OK}$$

Using the full expression demonstrates the member is (just) satisfactory. There are plenty of opportunities to make a mistake along the way, so careful attention to detail is important. Software will of course make the job easier. For manual calculations, the simplified versions of the expressions proposed by Mike Banfi are recommended, although it may be noted that there is not much more effort to complete the comprehensive expressions given in the Eurocode. A tool to verify members in combined bending and compression is available on *steelconstruction.info*, which may be used to confirm the results presented in the example.

References

1 Georgakis, M. Couchman, G, H.; Steel building design: Concise Eurocodes (P362); SCI, 2017

2 Manual for the design of steelwork building structures to Eurocode 3; The Institution of Structural Engineers, 2010

3 Banfi, M; Simplified expressions for compression and bending; The Structural Engineer, November 2008

The resistance of cross sections subject to shear and bending – theoretical analysis and practical design rules

Sections subject to both bending and shear have a reduced bending resistance where the shear force is greater than half the shear resistance. Richard Henderson of the SCI discusses the background and design rules.

Work carried out between 1930 and 1965 on the resistance of cross sections capable of being designed plastically was presented by Baker, Horne and Heyman[1]. Theoretical treatments of the effect of shear force on the resistance moment of sections were developed and were subsequently compared with tests. The design rules presented in BS 5950-1:2000 and subsequently in BS EN 1993-1-1 were based on this work.

Horne[2] examined rectangular and I sections and developed expressions for the reduction in the bending resistance of cross sections where the sections are subject to both bending and shear. In the examination, the sections are assumed to be capable of carrying their full plastic moment: sections are assumed to be restrained from global buckling and I sections are either class 1 or class 2 according to EC3.

Rectangular Section

A rectangular section will carry a bending moment equal to its elastic moment of resistance where only the extreme fibres reach yield stress. The remainder of the cross section is able to resist a shear force. The shear stress distribution is parabolic over the depth of the section and is zero at the extreme fibres with a maximum value at the neutral axis. The average shear stress is two thirds of the maximum value. If the bending moment is increased above the elastic moment of resistance, the area of the section available to resist shear is reduced until it vanishes when the plastic moment of resistance is reached. At this point, the whole section reaches its yield stress. The plastic resistance moment of the section is $M_p = (bh^2/4)f_y$ and its plastic shear resistance is $V_y = bh\tau_y$ if the bending and shear are each considered on their own.

When the bending moment is between the elastic and plastic moment of resistance, the elastic core of the section has a depth y_o above and below the neutral axis and $y_o < h/2$ where h is the depth of the section. The resistance moment is given by the sum of the plastic moment of resistance of the outer portion and the elastic moment of resistance of the core:

$$M = b/4(h^2 - 4y_o^2)\sigma_y + 2/3by_o^2\sigma_y$$

and the shear resistance is provided by the core and given by

$$V = 4/3by_o\tau_y.$$

Eliminating y_0 and using the expressions for M_p and V_p gives:

$$M_{pr}/M_p = 1 - 3/4(V/V_p)^2 \qquad (1)$$

M_{pr} is the reduced plastic moment of resistance in the presence of shear. The expression is valid for values of V up to that for which $y_o = h/2$ ie $V/V_p \leq 2/3$.

Horne showed that using the Tresca yield criterion, a less conservative estimate is given by $M_{pr}/M_p = 1 - 0.444(V/V_p)^2$ provided $V/V_p \leq 0.792$.

The interaction between shear and bending according to this expression is shown in Figure 1

According to the less conservative estimate, the bending resistance of the section is about 89% of the plastic resistance moment when the shear force is half the shear resistance.

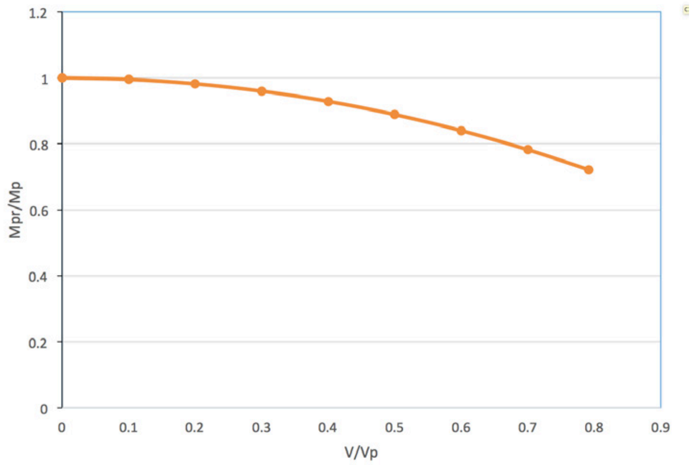

Figure 1: Interaction of shear and bending – Rectangular section

I Section

A similar analysis can be made of an I section, if the shear stresses are assumed only to be in the web. The plastic resistance moment of the web is denoted by $M_{pw} = (d_w^2t_w/4)\sigma_y$ and the shear resistance by $V_{pw} = d_wt_w\tau_w$, where d_w and t_w are the depth and thickness of the web. Using equation 1, the reduced plastic moment is given by:

$$M_{pr} = M_p - 3/4(V/V_{pw})^2 M_{pw}.$$

This equation is valid provided $V/V_{pw} \leq 2/3$ which means that the plastic zones in the section extend beyond the flanges and into the web.

Horne and Morris[3] discussed the effect of shear force on the plastic moment, assuming the web of the I section provides all the shear resistance and the shear stress τ_w is assumed to be uniform over the depth of the web. The longitudinal bending stress in the web is reduced because of the presence of the shear stress to a value which can be determined using the Von Mises yield criterion: $\sigma_w = [f_y^2 - 3\tau_w^2]^{0.5}$. The reduction in longitudinal bending stress in the web results in a reduced bending resistance given by:

$$M_{pr} = M_p - M_{pw}[1 - \{1 - (V/V_{pw})^2\}^{0.5}]$$

The interaction between the bending moments and the ratio of the applied shear force and shear resistance is shown in Figure 2.

The value of $(M_p - M_{pr})/M_{pw}$ where the shear force is half the shear resistance of the web is 0.134. The reduction in plastic bending resistance of the section is therefore about 13% of the plastic bending resistance of the web. For a 400 mm deep I section with 180 mm wide flanges 15 mm thick and an 8 mm thick web, the reduction in the full plastic bending resistance is only 3% under a shear force of half the shear resistance of the web. Figure 3 shows the relationship between plastic resistance moment and the ratio of shear force to shear resistance of the web for the I section discussed.

If bending about the minor axis of an I section is considered the behaviour is similar to a rectangular section and the shear stress is distributed parabolically over the width of the flanges and the bending stress distribution is also non-linear. The reduced bending resistance is given by Horne and Morris as:

$$M_{pr} = M_p[1 - 0.45(\tau_w/\tau_y)^2]$$

where τ_w is the shear stress calculated on the area of the flanges. If the shear force on the section is half the shear resistance of the flanges then the reduced resistance moment is about 89% of the full plastic resistance moment ie as found earlier.

Results of tests and design rules

Despite the foregoing analysis, the results of tests and also of advanced theory shows that there is no reduction in the resistance moment due to the presence of shear unless the shear force approaches the shear resistance of the section. This is because the portions of a beam section which are subject to both high shear and high bending stresses are limited in extent and are surrounded by elastic zones so plastic flow is largely prevented. The locations in a structure where both bending and shear may be significant are limited: the root of a cantilever and at the central support of a two–span beam are two possible locations.

The design rules in BS 5950-1:2000 and BS EN 1993-1-1 adopt a safe approach to the effect of shear force on the resistance moment and allow the full plastic resistance moment to be used in conjunction with a shear force of up to half the shear resistance of a beam. In fact BS 5950 was slightly more generous than EC3 and no reduction in bending resistance was required for shear force up to 60% of the shear resistance. The contribution of the shear area of the section to the bending resistance is reduced when the shear force on the section exceeds half the shear resistance. Figure 4 shows the percentage reduction in resistance moment according to both EC3 and BS 5950 for the 400 mm deep beam. The difference in the treatment is insignificant.

The reduction in minor axis bending resistance when the section is subject to a shear force is also shown in Figure 4, labelled Rectangular Section. Unlike the I section, the bending resistance reduces significantly under high shear and reduces to zero when the shear force reaches the shear resistance because the maximum shear stress of $f_y/\sqrt{3}$ is present over the full extent of the flanges. This effect also applies to rectangular sections. For a Tee section, the stem of the Tee provides the shear resistance but also develops longitudinal stresses to provide the bending resistance. These stresses are reduced in the presence of shear in a similar way to those in a rectangular section.

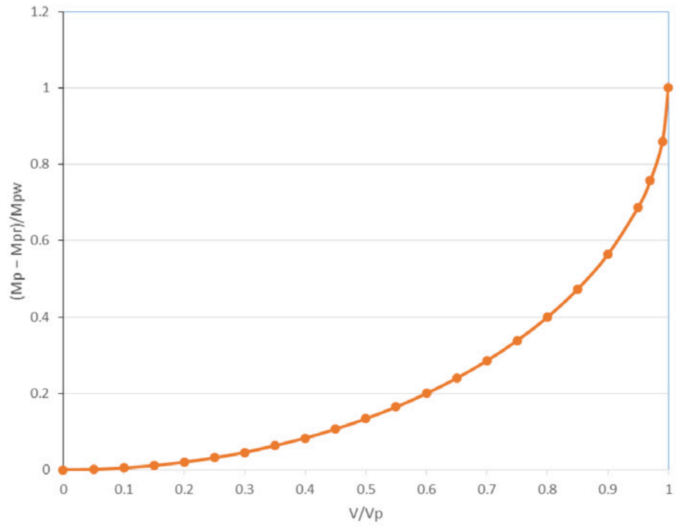

Figure 2 Effect of shear force on plastic moment of resistance of an I section

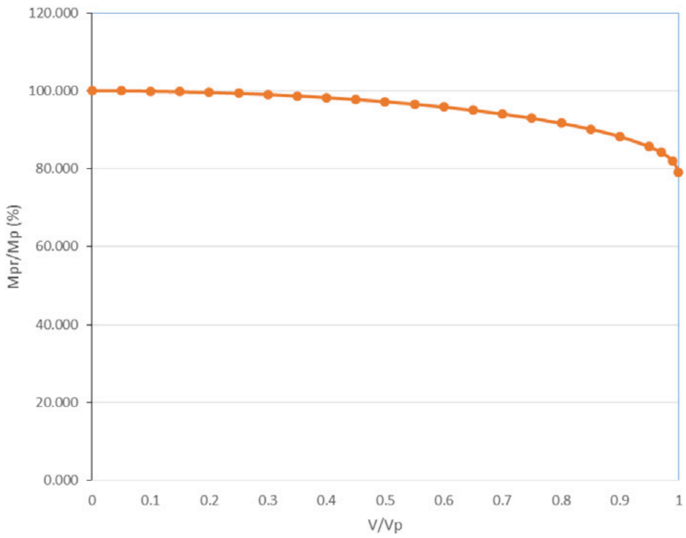

Figure 3 Reduction in plastic resistance moment for increasing ratio of shear force to shear resistance

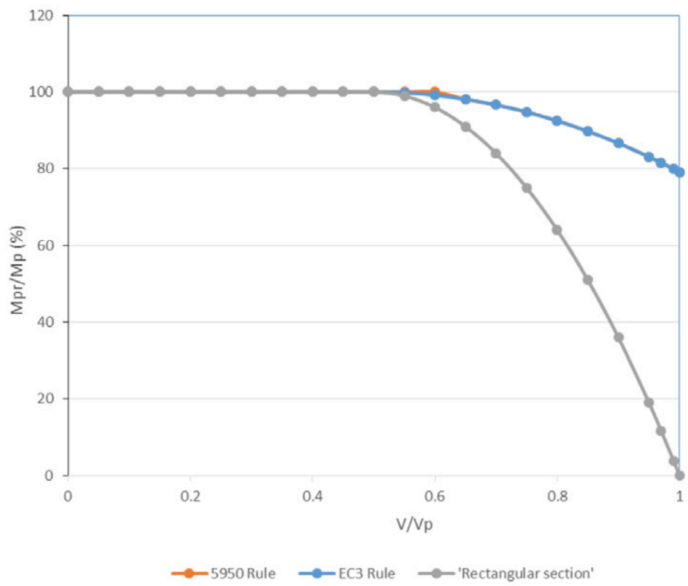

Figure 4 Reduction in resistance moment due to shear

References

1 Sir John Baker, M R Horne and J Heyman, The Steel Skeleton, Volume Two, Plastic behaviour & design, 1956, Cambridge University Press

2 M R Horne, Plastic theory of structures, 1979, Pergamon Press

3 M R Horne and L J Morris, Plastic design of low resistance rise frames, 1981, Granada Publishing

The use of S355 fin plates

Increasing interest in the use of S355 for fin plates prompted questions about the stiffness of such connections – are they still nominally pinned? David Brown of the SCI presents the results of the project comparing the behaviour of fin plate connections with both S275 and S355 fin plates.

Existing guidance

Rules for the design and detailing of fin plates were originally presented in the BS 5950 version of the Green Book[1]. At the time, fin plates were all from S275 material. Standardised connection details were presented, with design rules for each of the components. In support of the introduction of this type of connection to the UK, a series of physical tests were completed by Moore and Owens[2].

With any nominally pinned connection, ductility is required. One critical detailing rule to achieve ductile behaviour was therefore that either the supported beam web, or the fin plate, could be no thicker than *d*/2 in S275 material or 0.42*d* in S355 material. This rule was arranged that for Class 8.8 bolts, the bolt shear resistance (perceived as a relatively brittle failure mode) was no less than the bearing resistance – which was perceived as a ductile behaviour.

Thus for an M20 Class 8.8 bolt, according to BS 5950, the shear resistance is 92 kN

The bearing capacity for a bolt (assuming the end distance was not critical) is given by:

$P_{bs} = k_{bs} d t_p p_{bs}$

where:

k_{bs} = 1.0 for bolts in standard clearance holes

d is the bolt diameter

t_p is the thickness of the plate

p_{bs} = 460 N/mm² in S275 and 550 N/mm² in S355 (from Table 32 of BS 5950)

Thus for a 20 mm bolt in 10 mm thick S275 material, the bearing capacity is given by:

$P_{bs} = 1.0 \times 20 \times 10 \times 460 \times 10^{-3} = 92$ kN

If the material was S355, to ensure the shear resistance of the bolt is not critical, then

$$t_p < \frac{92 \times 10^3}{1.0 \times 20 \times 550} = 8.36 \text{ mm or } 0.42d$$

The advent of the Eurocodes

When the Eurocodes were introduced in 2005, two important changes had an impact on the rules for the design of fin plate connections. Firstly, the Eurocode demanded that the connections be formally classified – in the case of a fin plate to demonstrate that the connection was nominally pinned and secondly, the bearing resistance according to the Eurocode increased substantially.

Bearing resistance to BS EN 1993-1-8

According to BS EN 1993-1-8, the bearing resistance is given by:

$$F_{b,Rd} = \frac{k_1 \alpha_b f_u d t}{\gamma_{M2}}$$

If end and edge distance do not limit, then k_1 = 2.5 and α_b = 1.0. In 10 mm thick S275 material, with f_u = 410 N/mm² the bearing resistance for an M20 bolt becomes 164 kN, much higher than the BS 5950 value of 92 kN, and much higher than the bolt shear resistance, which according to the Eurocode is 94 kN for a Class 8.8 M20 bolt. Thus the previous rule to ensure ductility, that the bearing resistance should be less than the shear resistance, was impossible to meet in practice.

Connection classification to BS EN 1993-1-8

The Eurocode provided rules for the numerical calculation of connection stiffness, and a stiffness limit for nominally pinned connections. The rules are unfortunately only appropriate for end plate connections. Clause 5.2.2.1(2) also allows a joint to be classified on the basis of experimental evidence or evidence of previous satisfactory performance.

The Green Book to the Eurocode

In 2014, SCI and BCSA published the Eurocode Green Book[3]. The view taken was that there was both test evidence and significant previous experience to demonstrate that the standardised connections performed satisfactorily in practice, but that was conditional on the previous proven rules being followed. The Eurocode Green Book was at pains to point out that only the standardised connections were known to be satisfactory, and that varying the details might invalidate the proven behaviour. An important part of the limited scope was that the previous rules regarding fin plate or beam web thickness must be observed.

Changes to modern practice and the need for research

In recent years, the use of S355 has become more widespread, such that S355 is now the normal grade for rolled sections in the UK. In parallel, the use of S355 plate is becoming more common, and some steelwork contractors wished to use S355 fin plates. The limiting thickness of 8 mm was considered by many to be simply too thin – and so the need to assess the performance of fin plate connections with S355 plate was identified. The objective of the research was simply to compare moment-rotation and stiffness performance of fin plate connections. If connections with S355 fin plates were markedly stiffer than those with S275 plates, the classification as nominally pinned would be threatened.

Research programme

Firstly, an extensive desk study was undertaken to identify tests of fin plate connections. Physical test results are essential if the Finite Element (FE) model is to be calibrated – in other words to demonstrate that the FE model is a good model of the real behaviour. The test results must be comprehensive, as the measured properties of the components are needed, not just the nominal values. In addition, the results must be sufficiently detailed to allow a comparison of the moment-rotation behaviour. After reviewing the available test results, the original research by Moore and Owens[2] was the most comprehensive containing the necessary data.

For the connection chosen to calibrate the FE model, the comparison between the FE and the test results is shown in Figure 1.

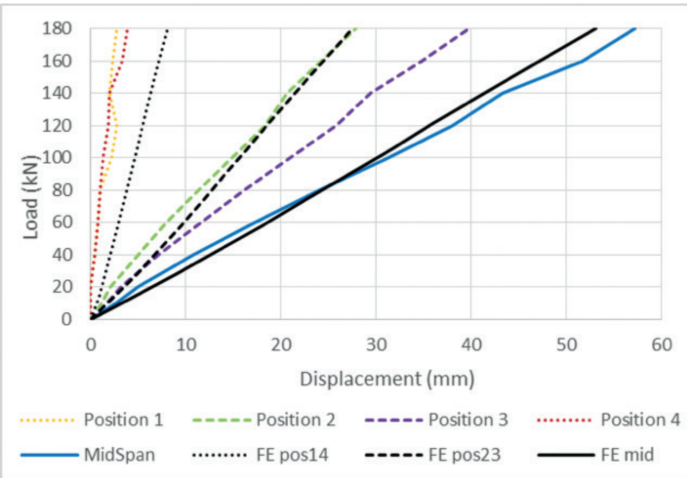

Figure 1: Comparison of FE and test results

In each case, the straight (black) lines in Figure 1 are the FE results, and illustrate deflection at points along the supported beam. The irregular lines show the measured deflections.

From Figure 1, it can be seen that the FE model was a good predictor of the test results. The stress patterns at the fin plate connection are shown in Figure 2. As anticipated, the higher stresses are at the extreme bolt locations in the fin plate. It should be noted that the stresses indicated are three-dimensional Von Mises stresses, so are not immediately comparable to (for example) a calculated bearing stress at a bolt location. The deformed shape of the fin plate (with an exaggerated horizontal scale) is also shown in Figure 2, and demonstrates behaviour as expected.

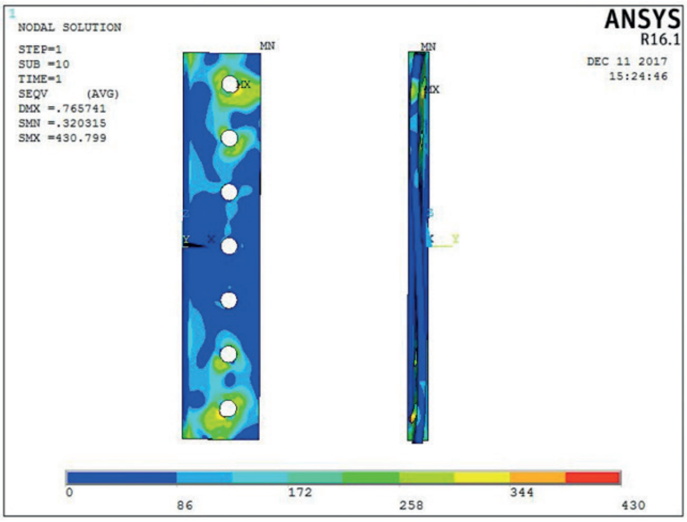

Figure 2: Stress diagram and deformed fin plate

Once the FE model was considered to provide a good model of the connection behaviour, a parametric study was undertaken, considering 28 different fin plate connections. Beams and connections were selected:

- with thin beam webs, so that the influence of the fin plate should not be significant,
- with thicker beam webs, so that the behaviour of the fin plate would be important,
- with one and two vertical columns of bolts,
- with a range of bolt rows.

In every case, the geometry of the standardised details shown in the Green Book was respected. Each case was analysed with a S275 fin plate and with a S355 fin plate.

Typical analysis results

Figure 3 shows the moment-rotation behaviour for the smallest connection considered – a 254 × 102 × 22 UB with just two bolts. Figure 3 also shows the limit for a nominally pinned classification, according to BS EN 1993-1-8. The connection is nominally pinned, and the moment-rotation plots are identical for S275 and S355 fin plates. This behaviour is expected, as the beam web is only 5.7 mm, so would be expected to be the critical component rather than the fin plate.

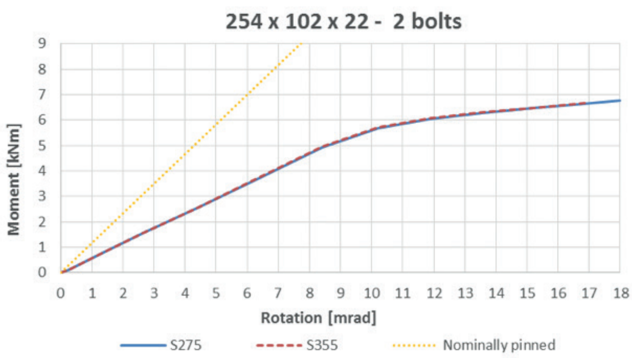

Figure 3: Moment-rotation curves for 254 × 102 UB, 2 bolts

Figure 4 shows the moment-rotation relationship for a 406 × 178 × 54 UB, with two vertical columns each of four bolts. Some small difference between the S275 and S355 fin plates is shown, at higher rotations. The initial stiffness is identical, and the connection would be classed as nominally pinned.

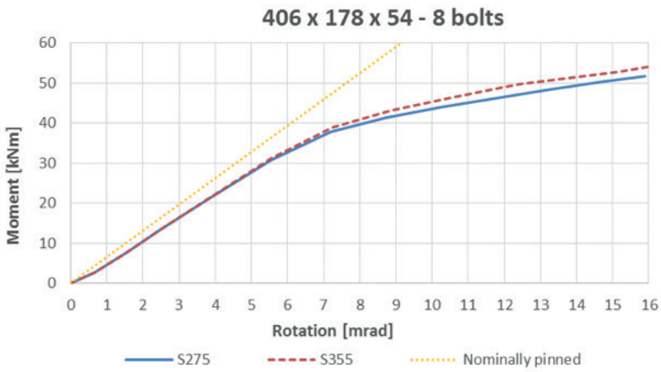

Figure 4: Moment-rotation curves for 406 × 178 UB, 8 bolts

The largest connection modelled was an 838 × 292 × 176 UB, with two vertical columns of 8 bolts. The web of this beam is 14 mm, so it would be expected that the behaviour would be dominated by the fin plate. The moment-rotation curves are shown in Figure 5. The connection is nominally pinned, with some increased stiffness at higher rotations with the S355 fin plate. It is suggested that the initial stiffness of the connection is dominated by deformation in bearing and that initially, this deformation is similar for both material grades.

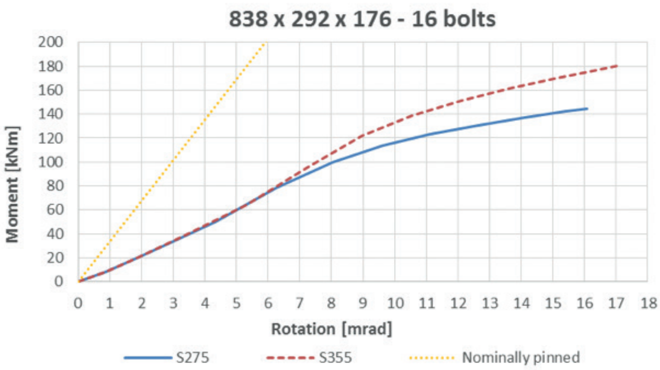

Figure 5: Moment-rotation curves for 838 × 292 UB, 16 bolts

Conclusions

The study has shown that as long as the standardised connection geometry presented in the Green Book[3] is respected, 10 mm fin plates in S355 are classed as nominally pinned connections and may be used as an alternative to S275 plates.

If the connection stiffness largely depends on the fin plate (i.e. the web of the beam is relatively thick), the connection stiffness for a given fin plate detail is similar and independent of the beam size. In contrast, the stiffness limit for a nominally pinned classification depends on the beam stiffness, which increases with the larger beams, making the nominally pinned classification more readily achieved for the larger sections.

One final observation is that the challenges of FE work should not be underestimated. This apparently straightforward study of a simple connection type involved contact surfaces, three-dimensional stresses, constraint by the bolts and plastic strains – reinforcing the need for calibration against physical tests.

Acknowledgements

This study was commissioned and funded by the BCSA and Steel for Life. The study was completed by Antonia Pilpilidou, formerly SCI.

References

1 Joints in steel construction. Simple connections (in accordance with BS 5950-1), (P212) "Green Book to BS 5950", SCI, 2009
2 Moore, D. B. and Owens, G. W., "Verification of design methods for fin plate connections", The Structural Engineer, Vol. 70, No.3/4 1992
3 Joints in steel construction. Simple joints to Eurocode 3, (P358) "Green Book", SCI, 2014

U-frames in bridges

Bridge designers will be familiar with compression flanges restrained by u-frames. David Brown of the SCI introduces the concept and illustrates the same principle commonly found in the design of portal frames.

Engineers are always concerned with the buckling of elements in compression and how restraint might be provided. In bridge construction and (for example) a twin truss span, it may be possible to brace between compression chords, as shown in Figure 1, to form an enclosed box.

Figure 1: Truss bridge with bracing between the compression chords

If bracing between the compression chords is to be avoided, some other means of restraining the compression chord (or compression flange, if the member is a beam) must be found. There are many examples of older footbridges where a horizontal cross member is extended laterally at deck level, and a diagonal brace provided to restrain the compression flange, as shown in Figure 2. People without an engineering background often think the metalwork was provided to support pipework (and it was often used for this), but the arrangement has a much more important function.

Figure 2: Bridges with external bracing to restrain the compression flange

Figure 3: "Half-through" bridge

With so-called "half-through" bridges, such as that shown in Figure 3, clearly no bracing is possible between the compression flanges. In this form of construction, the compression flanges are restrained by intermediate u-frames.

A typical cross section at a u-frame location is shown in Figure 4. A u-frame consists of a horizontal member (usually part of the deck steelwork) and vertical members. The connection between the horizontal member and the vertical member is continuous or semi-continuous forming a u-shaped stiff frame to provide restraint to the compression elements.

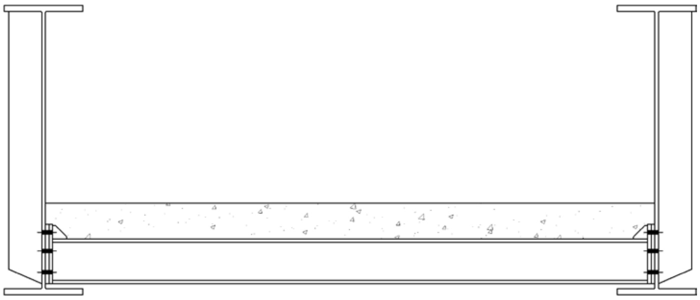

Figure 4: "Half-through" bridge typical cross section

Bridge design codes such as BS 5400-3 or BS EN 1993-2 allow designers to calculate an effective buckling length of the compression flange. The effective length primarily depends on the stiffness of the vertical members, the stiffness of the horizontal member and the stiffness of the connection between the members. Increased flexibility in the members or at the connections will lead to a longer buckling length. Detailed information on the design of half-through bridges, including the effect of u-frames, may be found on *steelconstruction.info*.

U-frames can also be seen in the footbridge pictured in Figure 5. In this form of construction, the compression flanges of the main girders are formed of square hollow sections, orientated as a diamond. Restraint to these compression flanges is provided by external u-frames fabricated from plate, which wrap around the bridge cross section at intervals along the span.

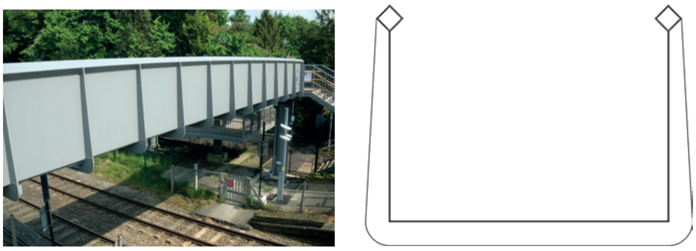

Figure 5: Footbridge with u-frames; cross section

Application in buildings

Although u-frames are associated with bridge construction, the same principle is found in portal frames, when the inside flanges of the members are restrained by bracing back to the purlins or side rails, as shown in Figure 6.

Some authorities (notably in other parts of Europe) consider this restraint system results in axial loads in the secondary steelwork, and that the restraint is only effective if purlins (or rails) assumed to provide restraint intersect with a node on the bracing (typically in the end bay). In the UK, there is no such

Figure 6: typical bracing to rafter

requirement and our understanding is that the torsional restraint is effective because of the u-frame action.

A section along a building is shown in Figure 7, along the line of a purlin, with inner flange restraints to a number of rafters. The compression in the inside flange would ordinarily result in lateral torsional buckling, with the purlins providing restraint to the tension flange only. Figure 7 shows that the rafters are restrained with respect to the purlin, forming an inverted u-frame.

Design requirements in portal frames

Two obvious requirements are clear from Figure 7. Firstly the purlin (or rail) must be continuous to be effective. If there is a break in the member, there is no u-frame action. This situation arises when side rails are interrupted, for example by a roller shutter door. In this case, short side rails between door jambs should not be relied on to provide restraint.

Secondly, as discussed in the context of bridges, the members of the u-frame must have appropriate stiffness. A traditional rule of thumb was to provide a side rail or purlin of at least 25% of the depth of the member being restrained. Horne and Ajmani proposed a rule to determine the necessary stiffness in 1973[1]. It is sobering to reflect that this rule was based on tests using members with tapered flanges and hot-rolled side rails, not the members typically used some 45 years later.

The rule considered the necessary restraint at a plastic hinge and may be expressed as:

$$\frac{I_s}{I_f} \geq \frac{f_y}{190 \times 10^3} \frac{B(L_1+L_2)}{L_1L_2}$$

where,

f_y is the design strength of the portal frame member
I_s is the second moment of area of the purlin or rail in its major axis
I_f is the second moment of area of the frame member
B is the span of the rail or purlin
L_1 and L_2 are the distances each side of the plastic hinge to the eaves or points of contraflexure, as shown in Figure 8.

As an illustration, for a rafter (Figure 8), and a span of 35 m, a reasonable assumption is that L_1 = 3.5 m and L_2 = 4 m

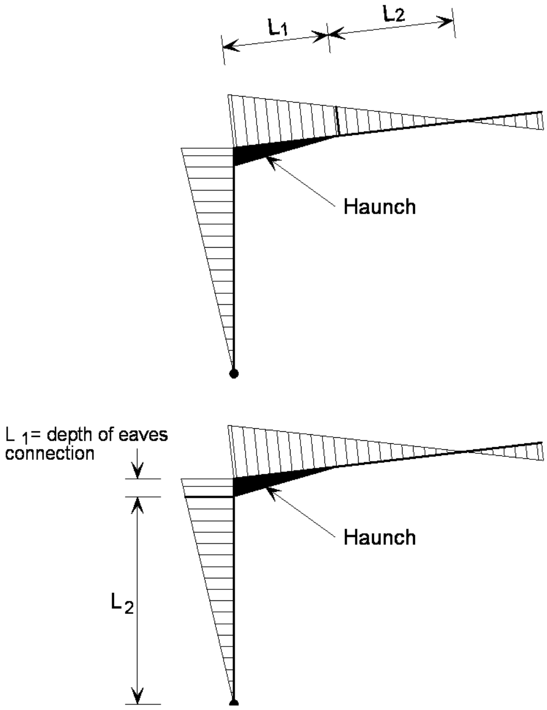

Figure 8: Lengths L_1 and L_2 used to check restraint member stiffness

Assuming the member is a 457 × 191 × 67 UB, then I_f = 29400 cm^4. If the rafter is S355 and the span of the purlin is 7 m, the stiffness requirement for the purlin becomes:

$$I_s \geq \frac{29400 \times 10^4 \times 355 \times 7000 \times (3500 + 4000)}{190 \times 10^3 \times 3500 \times 4000 \times 10^4} = 206\text{cm}^4$$

This order of inertia is provided by a 170 mm deep purlin, so normal frame arrangements appear to be adequate.

Unorthodox situations

The selection of purlins and side rails is normally made based on the span and loading on the member without any recourse to the check illustrated above. For orthodox construction, the relationship between the selected member and the stiffness necessary to provide u-frame action appears to be satisfactory. An issue can arise if the portal frames are long span, but nevertheless spaced at typical centres. Since the purlin (or rail) selection is based on the span and spacing of the secondary members, the purlins and rails selected for a long span frame may be the same as would be chosen for an orthodox span, but clearly the demands on stiffness are much higher.

The general advice is that orthodox frames with usual member sizes function satisfactorily with the 'normal' sizes and spacing of secondary steelwork. Situations where more care is needed are long span frames, and where the secondary steelwork is not continuous.

References

1 Horne, M, R and Ajmani, J,L.
Failure of columns laterally supported on one flange: Discussion
The Structural Engineer, Vol 50, No. 7, July 1973

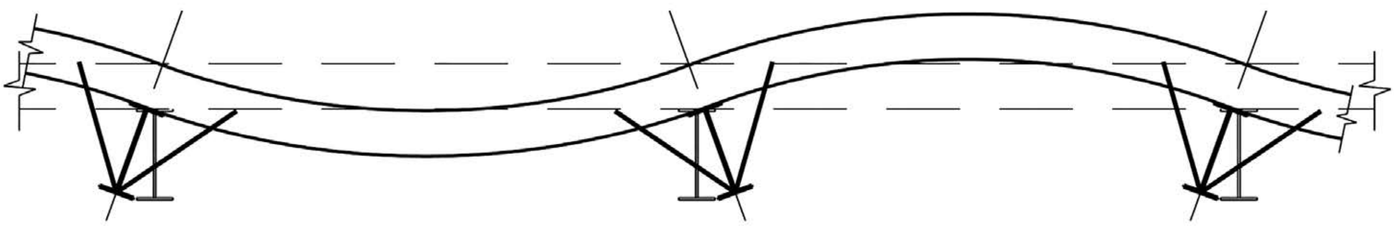

Figure 7: U-frame action in purlin restraint

Buckling resistance of uniform members in bending

Richard Henderson of the Steel Construction Institute discusses the phenomenon of lateral-torsional buckling.

Introduction

A grid of beams is usually divided into primary and secondary beams and where there is no floor slab to provide continuous support to the compression flanges, the secondary beams provide discrete restraints to the primary. An end plate connection to the primary beam web detailed in accordance with the Green Book rules may be considered to provide a fork end restraint. The secondary beams also apply point loads to the primary and, for this type of connection, the loads are not destabilizing. The system of point loads results in a shear force diagram for the primary beam with constant values between the point loads and a bending moment diagram made up of straight lines (ignoring the effect of the primary beam self-weight).

In determining the resistance of the beam to bending, especially in hand calculations, it is common to consider the primary beam in segments defined by the incoming secondary beams where the segments have defined end restraints and end moments taken from the bending moment diagram of the full beam. This approach corresponds to the conditions set out in clause 6.3.3 of Eurocode 3 which deals with uniform members in bending and axial compression and the effect of these two actions in combination. Note 1 to clause 6.3.3(2) states: "The interaction formulae are based on the modelling of simply supported single span members with end fork conditions and with or without continuous lateral restraints, which are subjected to compression force, end moments and/or transverse loads". Taking the segments one by one is usually on the safe side as the study described in the following sections shows. The purpose of the study is to determine what effect continuity of the beam beyond the segment being considered has on the beam's calculated bending resistance.

Beams studied

A series of loading arrangements on a 610 × 229 UB 140 was examined. All the arrangements were chosen to result in a 3 m segment of beam subject to a uniform moment of 1200 kNm. The point loads were always applied at restraint positions and beams of length 9 m and 15 m were considered. The loads and restraint positions were chosen such that the lengths of the segments were not always the same so that the half-wave lengths of the buckled shape were uneven. The arrangements are set out in Table 1.

Beam	Length (m)	No of point loads / restraints	Segment length (m)						
			1	2	3	4	5	6	7
1	9	2	3	3	3				
2	9	2	3.5	3	2.5				
3	15	4	3	3	3	3	3		
4	15	4	3.5	2.5	3	3.5	2.5		
5	15	6	2	2	2	3	2	2	2
6	15	4	3.5	2.5	3	2.5	3		

Table 1: Arrangement of beams and beam segments

As an illustration, the bending moment diagrams for beams 2 and 6 (neglecting the beam self weight) are shown in Figure 1.

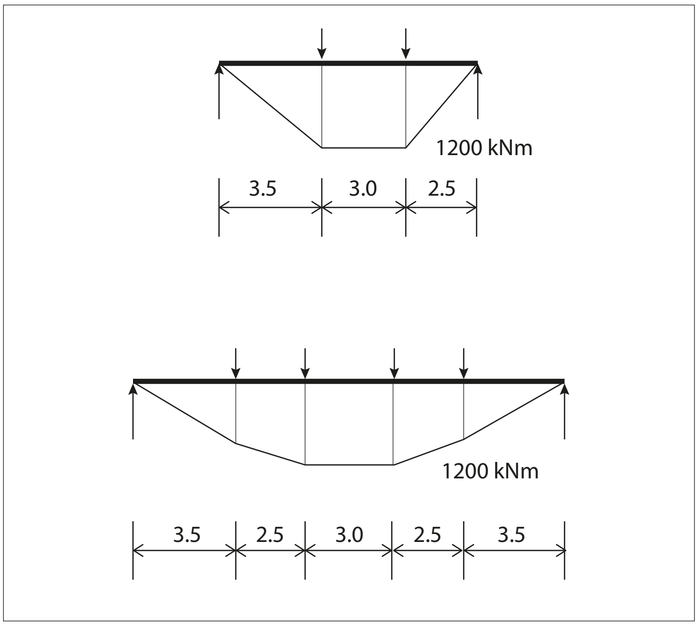

Figure 1: Bending moment diagrams, beams 2 and 6

Beams 1 and 3 have equally spaced loads and restraints, forming segments 3 m long. The buckled shape of the beam calculated by LTBeamN in determining M_{cr} is shown in plan in Figure 2. The top compression flange buckles into a series of half-waves. In each case, the central segment has a uniform bending moment and the adjacent segments have either triangular or trapezoidal-shaped bending moment diagrams. The amplitude of the half-waves can be seen to reduce where the bending moment is not uniform.

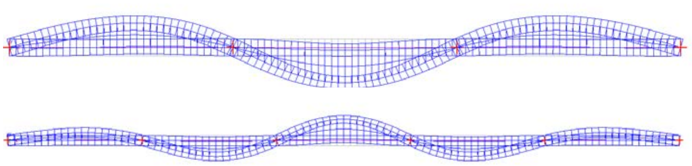

Figure 2: Buckled shape: 3-segment and 5-segment beams

Where the bending moment is uniform over the whole beam, the half-waves of the buckled shape can be seen to have the same amplitude as shown in Figure 3.

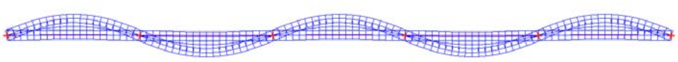

Figure 3: Buckled shape: 5-segment beam, uniform moment

Beam Resistances

The resistances of beam segments and beams identified in Table 1 have been calculated for comparison. The segments examined all have a maximum bending moment of 1200 kNm with a bending moment diagram which is either uniform or trapezoidal, except for the 9 m long beams where the bending moment diagram is triangular in the non-uniform moment segments.

The resistances have been determined using EC3 clause 6.3.2.3 for rolled section with the modified strength reduction factor $\chi_{LT,mod}$ from 6.3.2.5(2) and the UK National Annex. The correction factor k_c is determined from the C_1 factor where

$$C_1 = \frac{M_{cr}}{M_{cru}} \quad and \quad k_c = \frac{1}{\sqrt{C_1}}$$

M_{cru} is the elastic critical moment for a uniform moment on the segment. For interest, the unity factors are calculated for Beam 1 using the Blue Book method, by hand and by using LTBeamN to determine values of the critical moments. In addition to considering beam segments defined by the fork-end restraints, LTBeamN was used to analyse the whole beam and determine the critical moments for this case. The results are presented in Table 2.

For beam 1, the Blue Book, hand and LTBeamN methods reassuringly give unity factors which vary by 0.2%. The Blue Book approach probably differs from the other two because the tabulated values in the Book use 3 significant figures. All the 3 m long segments in the beams examined where the bending moment is uniform and equal to 1200 kNm are essentially the same with a unity factor of 0.982.

A closer examination of the results for the full length beams shows that beam 5 has the lowest unity factor of 0.840, about 85% of 0.982. The reduction in unity factor is due to the effect of the continuity of the beam on either side of the segment carrying the uniform bending moment; the continuity is obviously not present if the segments are considered alone. All the beams exhibit this effect to varying degrees. The spacings of restraints in beam 5 have been chosen to inhibit the twisting of the segment with the uniform moment as much as possible. A plan view of the buckled shape of beam 5 is shown in Figure 4. To illustrate the effect of continuity, the restraints are spaced at 2 m apart (except at the central segment), which may be considered unrealistically close spacing for secondary beams.

Beam 3 exhibits the highest unity factor, equal to 0.888 indicating that the continuity has the least effect. The spacing of the restraints are all equal at 3 m, allowing equal length half-waves. The buckled shape is shown in Figure 5.

The next highest unity factor 0.882 for Beam 4. The longer segment next to the segment with uniform moment allows a greater amplitude of lateral torsional distortion in the uniform moment segment. The buckled shape is shown in Figure 6

Beam	Segment	length (m)	method	M_{cr} (kNm)	M_{cru} (kNm)	unity factor
1	1	3.0	Blue Book	-	-	0.839
1	2	3.0	Blue Book	-	-	0.984
1	1	3.0	hand calc.	5964	3370	0.840
1	2	3.0	hand calc.	3370	3370	0.982
1	1	3.0	LTBeamN	6235	3366	0.840
1	2	3.0	LTBeamN	3365	3366	0.982
1	-	9.0	LTBeamN	4559	3366	0.866
2	1	3.5	LTBeamN	4709	2544	0.840
2	2	3.0	LTBeamN	3366	3366	0.982
2	3	2.5	LTBeamN	8759	4725	0.852
2	-	9.0	LTBeamN	4636	3193	0.841
3	2	3.0	LTBeamN	4029	3366	0.908
3	3	3.0	LTBeamN	3366	3366	0.982
3	-	15.0	LTBeamN	4263	3366	0.888
4	2	2.5	LTBeamN	5519	4729	0.867
4	3	3.0	LTBeamN	3366	3366	0.982
4	4	3.5	LTBeamN	3206	2544	0.941
4	-	15.0	LTBeamN	4251	3234	0.882
5	3	2.0	LTBeamN	7877	7223	0.840
5	4	3.0	LTBeamN	3366	3366	0.982
5	-	15.0	LTBeamN	6003	3365	0.840
6	2	2.5	LTBeamN	5430	4725	0.872
6	3	3.0	LTBeamN	3366	3366	0.982
6	-	15.0	LTBeamN	4725	3227	0.848

Table 2: Analysis results

Conclusion

For the beams examined, continuity of the element beyond the most highly loaded segment (that with a uniform bending moment of 1200 kNm) results in a lower unity factor than is exhibited when considering individual beam segments. For beam 5, the unity factor is reduced from 0.982 to 0.840, 85% of the value for the individual segment. The lower unity factor corresponds to a higher buckling resistance moment $M_{b,Rd}$ for the beam. For the cases where the secondary beam spacing is equal, the corresponding unity factors are 0.866 for a 9 m beam with two point loads and 0.888 for a 15 m beam with four point loads. The buckling resistance moments are calculated as 1351 kNm and 1385 kNm respectively, compared with 1220 kNm for the individual segment. Considering individual segments can therefore be seen to be on the safe side for all the arrangements considered and if extra resistance has to be squeezed out of an existing beam designed segment by segment because of a change in circumstances, an extra 10% could possibly be found by considering the beam as a whole.

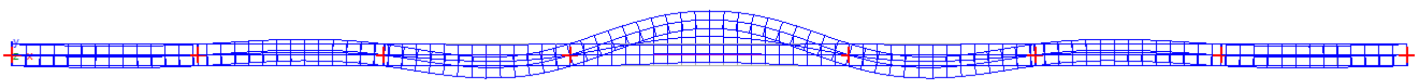

Figure 4: Beam 5 buckled shape

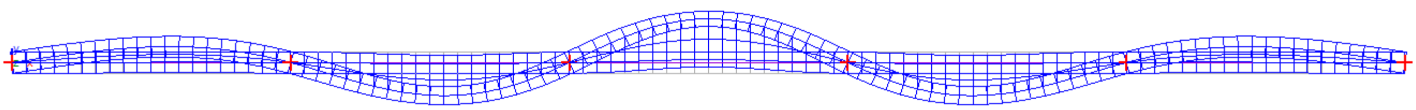

Figure 5: Beam 3 buckled shape

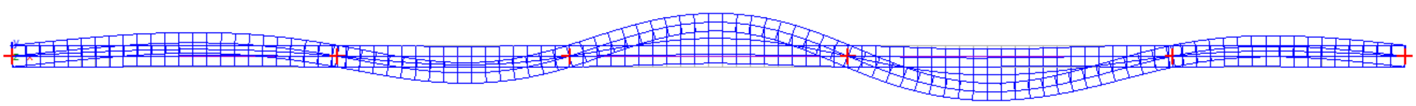

Figure 6: Beam 4 buckled shape

Introduction to fatigue design to BS EN 1993-1-9

The assessment of fatigue performance is routine in bridge design but is only relevant to specific elements in buildings which may suffer from fatigue damage. One example of these is crane runway beams. Richard Henderson of the SCI introduces some of the background.

Introduction

The phenomenon of metal fatigue involves the development of cracks in elements that are subject to many repeated applications of loads which are lower than the maximum loads to which the element is subjected. If fatigue cracks develop unnoticed, they will eventually result in complete failure of the element with potentially catastrophic consequences.

History

Research into fatigue in metal structures began as early as 1837 with tests on conveyor chains. A locomotive axle failure due to fatigue was recognized as the cause of a train accident at Meudon, near Versailles in 1842. F Braithwaite coined the term fatigue in his report "On the fatigue and consequent fracture of metals" published in the ICE minutes of proceedings in 1854. August Wohler conducted systematic investigations into metal fatigue of railway axles over a 20 year period from 1852, produced S-N curves illustrating fatigue behaviour and introduced the idea of an endurance limit. In 1945, A M Miner developed a design tool based on the Palmgren linear damage hypothesis. The stress raising effect of small-radius corners and the consequent effect on fatigue behaviour was established following investigation into the Comet air disasters of 1953 and 1954.

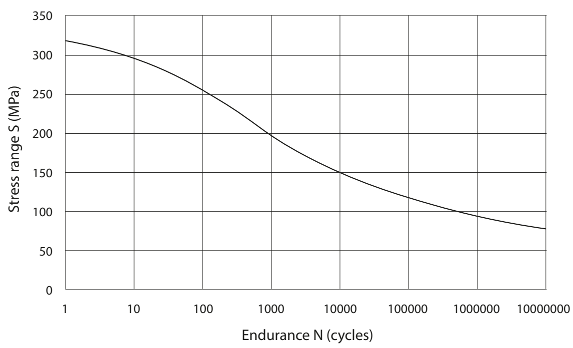

Figure 1: Example S-N Curve

Basic Concepts

Fatigue cracks usually initiate at a surface defect such as a sharp corner or a weld toe and develop when subject to fluctuating stresses above a certain threshold level. The endurance of a detail or component is the number of cycles to failure under a fluctuating stress of a constant amplitude. A point can be plotted on a graph with the number of cycles to failure (N) as abscissa and the constant amplitude stress (S) as ordinate. Stress range is defined as the algebraic difference between the two extremes of a stress cycle so the constant amplitude fluctuating stress is a constant stress range. By plotting the endurance for each constant stress range, a curve called an S-N curve can be drawn, the typical form of which is shown in Figure 1 on a semi-log plot.

The S-N curve exhibits a negative gradient such that a longer endurance corresponds to a lower stress range. Stresses below a stress range magnitude called the cut-off limit do not cause fatigue damage. According to Miner's rule, fatigue damage can be summed linearly for a given detail using the S-N curve to determine the number of cycles to failure N_i for stress range $\Delta\sigma_i$. If the detail is subject to a number of cycles n_i for the corresponding stress range, the fatigue damage can summed for k stress ranges and must be no greater than 1.0. The relevant expression is:

$$\sum_{i=1}^{k} \frac{n_1}{N_1} \leq 1.0$$

Defects in plain steel, welded joints and welded attachments all affect the fatigue life of a detail. As a result, many fatigue tests have been carried out on different details to develop S-N curves that can be used for fatigue damage calculations. Details are tabulated in BS EN 1993-1-9 (hereinafter denoted EC3-1-9) and are separated into the following headings.

Table No.	Heading
8.1	Plain members and mechanically fastened joints
8.2	Welded built-up sections
8.3	Transverse butt welds
8.4	Weld attachments and stiffeners
8.5	Load carrying welded joints
8.6	Hollow sections (t ≤ 12.5 mm)
8.7	Lattice girder node joints
8.8	Orthotropic decks – closed stringers
8.9	Orthotropic decks – open stringers
8.10	Top flange to web junction of runway beams

Within each table, details are identified and provided with an identifying number which corresponds to the relevant S-N curve.

The S-N curves for various classes of detail have been idealized in EC3-1-9 into a set of parallel lines with straight segments, plotted on a logarithmic scale on both axes and those for direct stress are shown in Figure 7.1 of the standard. The S-N curves are identified by a detail category number $\Delta\sigma_C$ which corresponds to the reference fatigue strength in MPa for the detail which is equal to the constant amplitude stress range for an endurance of 2×10^6 cycles. The curves are shown in Figure 2.

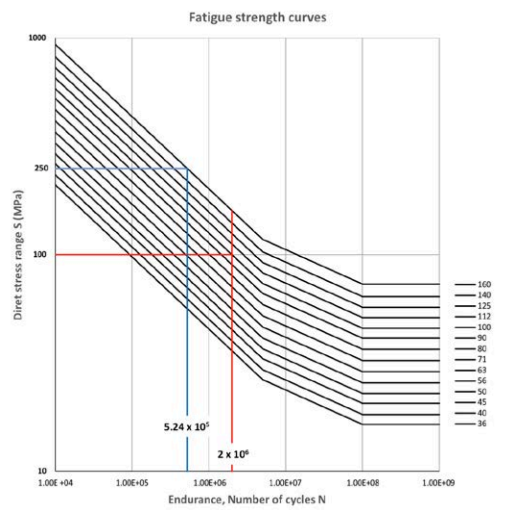

Figure 2: Fatigue strength curves for direct stress ranges

The equation for the sloping part of the curves is of the form:

$$\Delta\sigma_R{}^m N_R = \Delta\sigma_C{}^m 2 \times 10^6$$

with m = 3 for $N \leq 5 \times 10^6$ and:

$$\Delta\sigma_R{}^m N_R = \Delta\sigma_C{}^m 5 \times 10^6$$

with m = 5 for $5 \times 10^6 \leq N \leq 10^8$.

The first equation can be expressed as:

$$3 \times \log_{10}\Delta\sigma_R + \log_{10}N_R = 3 \times \log_{10}\Delta\sigma_C + \log_{10}2 \times 10^6$$

This is a straight line on a log-log plot with gradient -1/3. As an example of their use, for detail category 160 (plates and flats with as-rolled edges, with sharp edges, surface and rolling flaws removed by grinding until a smooth transition is achieved;

$\Delta\sigma_C = 160$ MPa – see Table 8.1 of EC3-1-9), the endurance for a nominal direct stress range of 250 MPa is given by:

$$3 \times \log_{10}250 + \log_{10}N_R = 3 \times \log_{10}160 + \log_{10}2 \times 10^6$$

$$N_R = 5.243 \times 10^5$$

ie the endurance at a constant amplitude stress range of 250 MPa is about 524,000 cycles.

Fatigue loading

Fatigue loading usually involves a spectrum of loads of different magnitudes. A spectrum can be built up for a particular structural action which can then be converted into a stress history.

A method for determining the magnitude of stress ranges from a stress history is known as the reservoir counting method and is described in Published Document PD 6695-1-9:2008.

The reservoir counting method is illustrated in Figure 3.

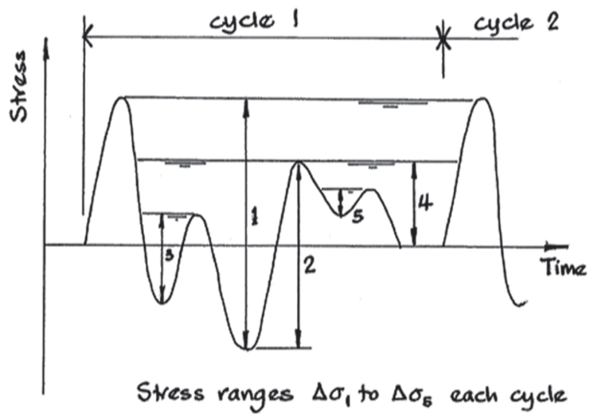

Figure 3: Reservoir counting method

The load spectrum may be continuous (such as for wave loading) and be describable by fitting a probability distribution to measured data. The data can then be discretized and a histogram of the number of loads of different magnitudes produced. The stress ranges corresponding to each load magnitude can then be determined.

Fatigue Assessment and Verification

Two methods of fatigue assessment are described in EC3-1-9: the safe life method and the damage tolerant method. The safe life method of assessment is considered in what follows. For some circumstances, a simple method of fatigue assessment can be used which does not refer to a load spectrum. The method is set out in EC3-1-9 and involves verification in the stress domain; it is described below.

Sections 5 and 6 of the standard provide details of how to calculate the stresses for assessing the fatigue performance of a detail. Nominal values of stresses should be calculated at the serviceability limit state according to elastic theory, excluding stress concentration effects. The nominal direct and shear stresses should be calculated at the site of potential initiation of a fatigue crack. The nominal stresses are modified by a stress concentration factor if the relevant nominal stress is affected by a local geometric feature, such as an opening with radiused corners. Stress concentration factors are provided in Figure 4 of PD6695-1-9:2008. Stresses in welds are calculated using a different formula from that given in BS EN 1993-1-8 for weld design, as indicated in Section 5(6). For certain details shown in Table B.1 of EC3-1-9, fatigue resistance can be determined using the geometrical (hot spot) stress method. Stress ranges for fatigue design are based on nominal stresses, modified nominal stresses or geometrical (hot spot) stress ranges.

For the structure and loading under consideration, the relevant part of EN 1993 may provide parameters for calculating the design value of the nominal stress ranges for fatigue verification. Using this approach, the design value of the nominal, modified nominal or geometrical stress range factored for fatigue must be less than the reference fatigue strength at 2 million cycles for each detail identified in tables 8.1 to 8.10.

The design value of nominal stress ranges is given in Section 6.2 of EC3-1-9 as

$$\gamma_{Ff}\,\Delta\sigma_{E,2} = \lambda_1 \times \lambda_2 \times \lambda_3 \times \lambda_4 \ldots \times \lambda_n \times \Delta\sigma(\gamma_{Ff}\,Q_k)$$

for direct stresses where $\Delta\sigma(\gamma_{Ff}\,Q_k)$ is the stress range caused by the fatigue loads specified in EN 1991 and the λ_i are damage equivalent factors depending on the spectra in the relevant parts of EN 1993. The product of the damage equivalent factors λ_i adjusts the stress ranges caused by the fatigue loads into stress ranges corresponding to 2×10^6 cycles.

The fatigue verification involves checking that the nominal, modified nominal or geometrical stress ranges due to frequent loads $\Psi_1 Q_k$ do not exceed the following limits:

$$\Delta\sigma \leq 1.5f_y \quad \text{for direct stress ranges}$$

$$\Delta\tau \leq (1.5f_y)/\sqrt{3} \quad \text{for shear stress ranges}$$

Under fatigue loading, the following two inequalities should be verified:

$$\frac{\gamma_{Ff}\Delta\sigma_{E,2}}{\Delta\sigma_C/\gamma_{Mf}} \leq 1.0$$

$$\frac{\gamma_{Ff}\Delta\sigma_{E,2}}{\Delta\tau_C/\gamma_{Mf}} \leq 1.0$$

The design value of the nominal stress ranges should therefore be less than the reference fatigue strength at 2 million cycles for that particular detail.

In addition, for stress ranges of combined shear and direct stress a further inequality should be satisfied:

$$\left(\frac{\gamma_{Ff}\Delta\sigma_{E,2}}{\Delta\sigma_C/\gamma_{Mf}}\right)^3 + \left(\frac{\gamma_{Ff}\Delta\sigma_{E,2}}{\Delta\tau_C/\gamma_{Mf}}\right)^5 \leq 1.0$$

Lambda values which allow this approach are given in BS EN 1991-3 for cranes and in BS EN 1993-2 for bridges.

UK National Annex

The UK National Annex to EC3-1-9 states that where no λ_i values are given the relevant parts of EC3, the verification should be based on the damage accumulation equation which is essentially the equation for Miner's rule:

$$D_d = \sum_{i=1}^{n} \frac{n_{Ei}}{N_{Ri}} \leq 1.0$$

The most comprehensive load model available should be used to establish a spectrum of stress ranges. The spectrum consists of a series of bands of stress $\Delta\sigma_i$ which should be multiplied by the load factor γ_{Ff}. The reference fatigue strength values $\Delta\sigma_C$ divided by γ_{Mf} are used to obtain the endurance value N_{Ri} for each band.

In the equation for damage, n_{Ei} is the number of cycles associated with the stress range $\gamma_{Ff}\,\Delta\sigma_i$ for band i in the factored spectrum and N_{Ri} is the endurance in cycles obtained from the

factored $\dfrac{\Delta\sigma_C}{\gamma_{Mf}} - N_R$ curve for a stress range of $\gamma_{Ff}\,\Delta\sigma_i$.

It is intended to give a more detailed discussion of a fatigue check in an example in a subsequent article.

Temperature profiles through composite slabs at elevated temperatures

Callum Heavens of the SCI discusses different methods for determining temperature profiles through composite slabs at elevated temperatures.

Introduction

The resistance of composite slabs at elevated temperatures is dependent on the temperatures that the critical regions of the slab reach within a given period of time. The strength of the steel in the deck, and in any bar or mesh reinforcement, reduces with temperature, as does the strength of the concrete within the slab. It is imperative that the temperatures of these components be determined accurately when designing the slab in order to satisfy the requirements of a given fire resistance period.

The temperature profile through the slab is dependent on the depth into the slab from an exposed surface but determining exact temperatures at a given depth is complicated by the shape (re-entrant or trapezoidal) and dimensions of the deck profile, as well as the moisture content of the concrete.

The components contributing to the sagging and hogging resistance of the slabs will depend on the particular design method being employed (such as the "Mesh & Deck" method or the "Bar" method). However, regardless of the chosen method, the temperature is obtained by a temperature profile which may be tabulated or given by equation.

BS 5950-8[1] and BS EN 1994-1-2[2] provide tabulated temperature data for light and normal weight concretes for different fire resistance periods, whilst NCCI document PN005c[3] provides a set of calibrated equations which give temperature as a function of depth, considering the fire period and concrete type. By determining the temperature at the location of interest, the reduction in strength of the material can then be evaluated for British Standard design using BS 5950-8 Table 1 to Table 3 or for Eurocode design using BS EN 1994-1-2 Table 3.2 to Table 3.4.

BS 5950-8

Fire resistant design to British Standards is given in BS 5950-8:2003, with composite slabs being discussed in Section 8.9.

Here, the temperature profile through a 100mm composite floor slab with a profiled steel deck is given in Table 12. This table provides temperatures at 10mm intervals through the slab for both normal and lightweight concretes and for fire resistance periods in steps of 30 minutes from a minimum duration of 30 minutes up to a maximum duration of 240 minutes.

This data is plotted in Figure 1 for normal weight concrete. BS 5950-8 only provides temperature data up to a maximum temperature of 800°C. No distinction is made between the temperature profiles of re-entrant or trapezoidal slab decks. Instead, it is stated that the temperature relates to a location at the prescribed distance from the nearest exposed surface, whether that be the deck soffit, rib wall or top of a re-entrant dovetail.

No limits are placed on the scope of this tabulated data, however, the limits on the applicability of the insulation criteria should be noted.

BS EN 1994-1-2

The temperature model for composite slabs in the Eurocodes is given in BS EN 1994-2:2005 Annex D. This annex provides methods for separately considering the thermal insulation requirements, the sagging resistance and the hogging resistance.

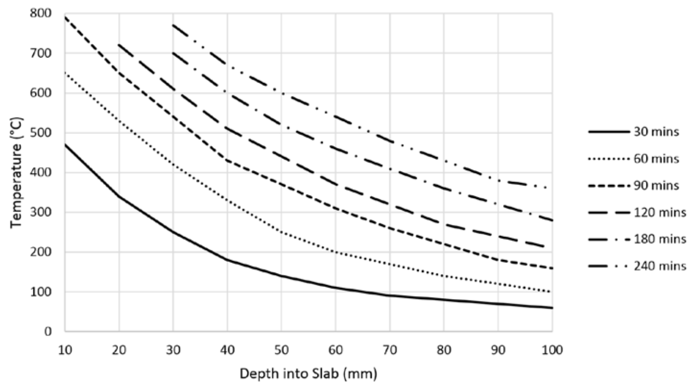

Figure 1: Temperature profiles through a 100mm composite slab according to BS 5950-8 for normal weight concrete.

As part of determining the hogging resistance, Table D.5 provides tabulated temperature data throughout a 100mm slab for fire durations of 30 to 240 minutes for normal weight concrete (it is stated that for lightweight concrete, the temperatures should be reduced to 90% of the normal weight values). As with BS 5950-8, only temperatures up to 800°C are presented in the table.

The use of this table differs slightly from BS 5950-8 in that the depth is measured from the base of an "effective slab height" which is equal to the cover depth of concrete above the deck in addition to some portion of the rib height (determined by the rib dimensions).

The scope of this data is limited by a set of dimensional requirements which are given in Table D.7 of Annex D.

Annex D is an informative Annex. Its use is determined by the National Annex[4] which states that it "should not be used" with "alternative guidance given" by "reference to non-contradictory complementary information".

NCCI PN005c

PN005c is non-contradictory complementary information that provides an alternative to the guidance presented in Annex D of BS EN 1994-1-2. Rather than provide tabulated data as in the case of BS 5950-8 and BS EN 1994-1-2, the NCCI provides three calibrated equations for determining the temperature profile through a composite slab for each of normal and lightweight concrete.

The equations are quadratic curves fitted to data obtained from a combination of physical test results and finite element (FE) results calibrated against these tests. The temperature profile within the width of the rib (i.e. over the full slab depth) is described by two curves. The first curve applies over the first 80mm above the deck soffit and the second applies to the remainder of the slab depth. Over the reduced depth of the slab, the profile is described by a third curve.

The coefficients of each of these quadratics are tabulated for fire resistance periods of 30, 60, 90 and 120 minutes, with some of these values dependent on parameters determined by the profile height, slab depth or trough width. These equations lead to temperature distributions through the slab of the general form illustrated in Figure 2. Different coefficients are presented depending on whether the deck is re-entrant or trapezoidal.

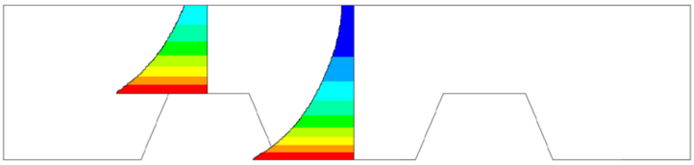

Figure 2: Illustration of a typical temperature distribution through a composite slab.

The slab can be divided into a number of thin horizontal strips whose temperatures can then be determined using the equations discussed previously. The temperature of any mesh reinforcement can be determined from the temperature of the concrete strip at the level of the mesh. Separate equations are given for determining the temperature of bar reinforcement.

In addition, by applying these equations to a number of locations along the top surface of the slab, the acceptability of the slab with regard to the insulation criteria (also specified in PN005c) can be determined by evaluating the maximum and average temperature rises along this surface. A typical surface temperature profile is shown in Figure 3.

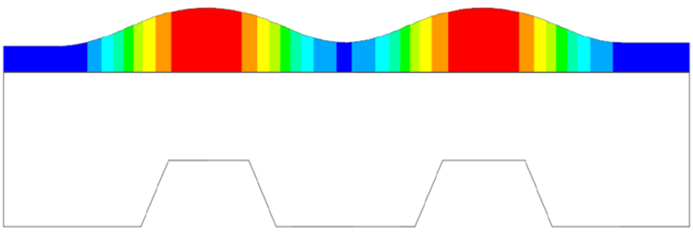

Figure 3: Illustration of a typical temperature distribution along the surface of a composite slab

The scope of PN005c is limited to a specified range of deck geometries, however, this range covers the majority of deck profiles available within the UK. For trapezoidal decks, the profile height is required to be in the range 60-80mm whilst the bottom flange width should be between 100-130mm. For re-entrant decks, the profile height should be in the range 50-60mm and the bottom flange width in the range 120-150mm.

Profile Comparisons

Figures 4 and 5 show a comparison of the temperature profiles given in BS 5950-8, BS EN 1994-1-2 and PN005c for fire resistance periods of 90 minutes and 120 minutes respectively. The profiles are plotted for a typical 60mm trapezoidal deck with a bottom flange width of 125mm and a total slab depth of 140mm. The profiles are also plotted against physical test data obtained from tests on a slab of the same geometry and the results of an FE analysis. All data is for normal weight concrete.

It can be seen that BS 5950-8 and BS EN 1994-1-2 provide very similar profiles. However, at some depths into the slab, both profiles are un-conservative when compared to the physical test data. This is even more noticeable for the 120 minute fire resistance period where temperature differences can be as high as 100°C.

It would appear on first inspection that PN005c produces overly conservative results. However, it should be noted that these equations are required to take account of a range of deck and slab geometries. The PN005c curves provide an envelope on the actual temperature profile through the composite slab in all of these cases.

The FE results tend to provide relatively good agreement with the test data, being slightly conservative in most cases. Where the FE results are un-conservative, they indicate only very slightly lower temperatures than the test data. In cases where a deck or slab geometry falls outside of the scope of the codes or PN005c, FE analysis is an accurate alternative for determining an appropriate temperature distribution through a composite slab and is especially useful for profiles of unusual geometry.

Conclusions

1. BS 5950-8 and BS EN 1994-1-2 provide tabulated data for temperature profiles which in some cases can be un-conservative. The two codes produce very similar temperature profiles but the UK National Annex does not allow the use of the profiles provided in BS EN 1994-1-2.
2. PN005c provides a set of calibrated quadratic equations to describe the temperature profile in different locations within a composite slab. It takes account of a range of deck geometries to provide safe temperature profiles.
3. FE analysis is a suitable alternative to the curves presented here and is particularly suited to unusual deck profiles which may fall outside the scope of the codes and NCCI document.

The follwing article considers how the temperature profile through the slab can be used in the design of composite beams in fire.

References

1 BS 5950-8:2003
Structural use of steelwork in building - Part 8: Code of practice for fire resistant design
BSI, 2003

2 BS EN 1994-1-2:2005
Eurocode 4 - Design of composite steel and concrete structures - Part 1-2: General rules - Structural fire design
BSI, 2005

3 PN005c-GB
NCCI: Fire resistance design of composite slabs
The Steel Construction Institute

4 NA to BS EN 1994-1-2:2005
UK National Annex to Eurocode 4: Design of composite steel and concrete structures - Part 1-2: General rules - Structural fire design
BSI, 2008

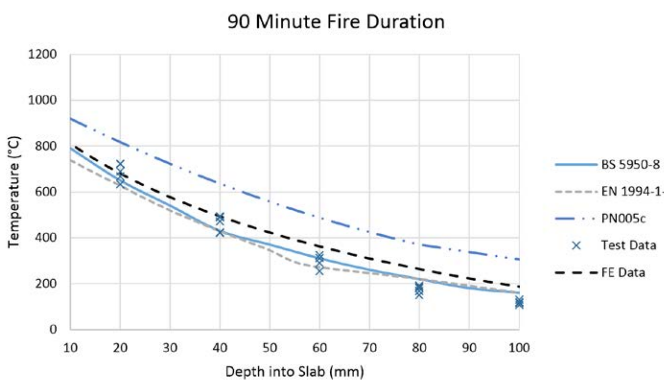

Figure 4: Comparison of temperature profiles for a 90 minute fire (using normal weight concrete)

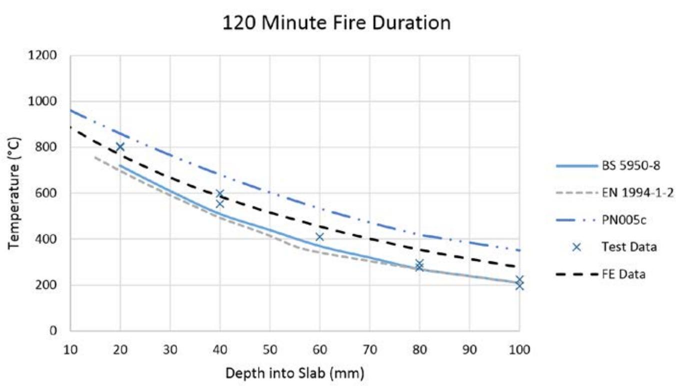

Figure 5: Comparison of temperature profiles for a 120 minute fire (using normal weight concrete)

Composite beam design at elevated temperature: comparisons between different temperature distributions in the concrete flange

Several resources give guidance on the temperature profile through composite slabs; BS 5950-8, EN 1994-1-2 and NCCI PN005C-GB. Ricardo Pimentel of the SCI discusses the impact of these alternative profiles on the design of composite beams at elevated temperature.

Composite beams are one of the most common structural elements in the UK construction market. Steel and concrete are connected by mechanical devices (shear connection – usually studs), allowing the two materials to work together. Composite beams are usually simply supported elements, allowing the steel to be mainly in tension and the concrete in compression.

The fire design of composite beams is often required, which demands an assessment of resistance of the concrete, steel and studs at elevated temperature. The main topic of this article is to evaluate the impact of alternative temperature distributions in the slab to obtain the critical temperature or the allowable fire exposure period of composite beams. For a composite beam design at elevated temperature, there are three possible ways to model the temperature distribution in the slab in the UK: (i) EN 1994-1-2[1] Annex D Table D.5; (ii) BS 5950-8[2] Table 12; (iii) NCCI PN005C-GB[3]. However, note that the UK National Annex to EN 1994-1-2[4] states that Annex D should not be used, recommending the use of non-contradictory complementary information (NCCI).

The effect of different temperature profiles will be assessed based on two worked examples, comprising 6 m and 12 m span beams, both optimized for an adequate performance under Serviceability Limit States, Ultimate Limit States and Fire Design. The geometry and design conditions for the two worked examples are summarized in the data presented in Figure 1 and Table 1.

According to EN 1994-1-2, to take into account the ribs of a trapezoidal deck, an effective slab depth can be calculated (h_{eff} - Figure 1), allowing a more realistic uniform temperature distribution in the concrete flange. According to equations D.15a and D.15b of EN 1994-1-2, an effective depth of 100 mm can be obtained for the slab shown in Figure 1 (h_{eff} = 100 mm). Basically, this effective depth means that the temperature of the top concrete fibre is obtained assuming a depth of 100 mm in table D.5 of EN 1994-1-2.

There are no recommendations in the NCCI or BS 5950-8 for assessing an effective slab depth for composite floors. When estimating the resistance of the concrete flange at elevated temperature using NCCI, a weighted average between temperatures above ribs and between ribs can be considered (using l_2 and l_3 to calculate the weighted average). If BS 5950-8 is used, the approach of equations D.15a and D.15b of EN 1994-1-2 can be assumed to be valid. An alternative (and conservative) measure can be to disregard the ribs, i.e., assuming that h_{eff} = h_1 = 70 mm.

The temperature on the unexposed (top) side of the slab is required to be no more than approximately 140°C to fulfil insulation requirements[5]. A minimum slab thickness is imposed to fulfil this requirement. For the beam analysis, according to EN 1994-1-2, 4.3.4.2.2 (16), it may be assumed that for concrete temperatures below 250°C, no strength reduction is necessary. For these reasons, according to some references[6], assuming room temperature

h_1 [mm]	70
h_2 [mm]	60
l_1 [mm]	175
l_2 [mm]	125
l_3 [mm]	125

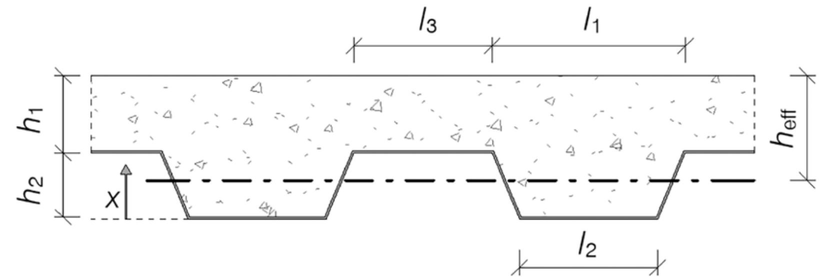

Figure 1 – Composite slab geometry.

Characteristic	Description/value
Steel section for the 6 m beam:	UB 203 x 133 x 25
Steel section for the 12 m beam:	UB 406 x 178 x 67
Effective slab breath to 12 m span:	3000 mm
Effective slab breath to 6 m span:	1500 mm
Floor usage:	Office
Beam spacing [m]	3.50
Slab weight [kN/m²]	2.65
Additional permanent loads [kN/m²]	2.00
Imposed Load [kN/m²]	2.70
Steel:	S355 JR
Concrete:	C30/37
Slab mesh:	A142
Ribs direction:	Perpendicular to the steel beam.
Fire protection:	Yes
Temperature gradient:	Uniform temperature in the steel profile.
Fire rating:	90 minutes
Steel Critical temperature – 6 m span:	620°C
Steel Critical temperature – 12 m span:	621°C
Miscellaneous:	Cambered beam; restrained by steel sheet in construction stage.

Table 1 – Design conditions

Case	Methodology (90 minutes of fire exposure)	$\theta_{c,top}$	K_c
1	Room Temperature	20	1.00
2	EN 1994-1-2 Annex D (h_{eff} = 100 mm)	160	0.97
3	BS 5950-8 with EN 1994-1-2 Annex D (h_{eff} ≥ 100 mm)	160	0.97
4	Medium value according to NCCI (weighted average)	224	0.93
5	Ignoring Ribs According to EC (h_{eff} = 70 mm)	246	0.90
6	Ignoring Ribs According to BS 5950-8 (h_{eff} = 70 mm)	260	0.89
7	Ignoring Ribs According to NCCI (h_{eff} = 70 mm)	244	0.91
8	Assuming 40% of steel top flange temperature (θ_{top} flange = 620°C) EN 1994-1-2, 4.3.4.2.5 (2) – for shear studs resistance.	248	0.90

Table 2 – Top concrete fibre temperature according to different approaches (X = 130 mm).

Case	Methodology (90 minutes of fire exposure)	$\theta_{c,top}$	K_c
1	Room Temperature	20	1.00
2	EN 1994-1-2 Annex D (h_{eff} = 100 mm)	428	0.71
3	BS 5950-8 with EN 1994-1-2 Annex D (h_{eff} ≥ 100 mm)	430	0.71
4	Medium value according to NCCI (weighted average)	559	0.51
5	Ignoring Ribs According to EC (h_{eff} = 70 mm)	738	0.24
6	Ignoring Ribs According to BS 5950-8 (h_{eff} = 70 mm)	790	0.17
7	Ignoring Ribs According to NCCI (h_{eff} = 70 mm)	747	0.23
8	Assuming 40% of steel top flange temperature (θ_{top} flange = 620°C) EN 1994-1-2, 4.3.4.2.5 (2) – for shear studs resistance.	248	0.90

Table 3 – Bottom concrete fibre temperature according to different approaches (X = 60 mm).

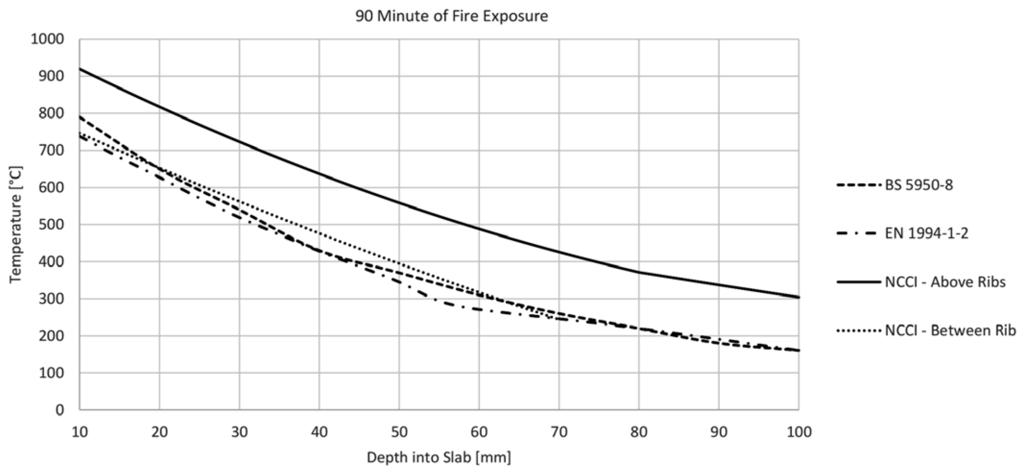

Figure 2 - Temperature distribution according to different UK resources.

to Figure 1). Eight possible approaches are presented. Once the temperatures have been obtained, the respective concrete resistance reduction factors (K_c) according to Table 3.3 of EN 1994-1-2 can be obtained. In the top concrete fibres, according to EN 1994-1-2 and BS 5950-8 approaches, the top temperature is in fact close to 140°C (Cases 2 and 3). Even with conservative approaches (Cases 5, 6 and 7), the temperature in the top concrete fibre is generally below 250°C, so no concrete strength reduction would be needed for the top concrete fibres. On the other hand, for lower concrete fibres, the strength reduction can be up to 29 % for Cases 2 and 3 and 83 % for Case 6. Thus, depending of the depth of the concrete flange required for section equilibrium, the concrete resistance may have some significant reductions.

To evaluate the impact of different temperature distributions in the slab, the critical steel temperatures shown in Table 1 were assumed as fixed. The plastic bending resistance under fire, for each slab profiles temperatures (Cases 1 to 8) were then evaluated, and are presented in Table 4 and Table 5 (overleaf) for the two worked examples. The degree of shear connection (η) can vary between 0 and 1 in a composite beam. Results for different degrees of shear connection are presented in steps of 0.25 between those two extreme cases, obtained through a stress block analysis. Partial interaction curves are presented for both worked examples in Figure 3, for 6 m and 12 m worked examples.

for assessing the sagging bending resistance of composite slabs and beams is suggested, as, in general, only a modest depth at the top of the slab will be necessary to obtain section equilibrium at elevated temperature. Thus, an example assuming room temperature in the slab will also be considered (note that if floor screed is considered for the minimum insulation thickness, the temperature in the top concrete fibre can be slightly higher).

For 90 minutes of fire exposure, the minimum insulation thickness according to EN 1994-1-2 Annex D would be h_{eff} ≥ 100 mm (note that the profile falls outside the scope of Annex D of EN 1994-1-2, which limits l_3 to 115 mm, compared to the actual value of 125 mm). According to the NCCI, a minimum thickness of h_1 ≥ 70 mm is imposed, while BS 5950-8 suggests h_1 ≥ 70 mm for lightweight concrete and h_1 ≥ 80 mm for normal weight concrete.

In Figure 2, for 90 minutes of fire exposure, the different temperature distributions in the concrete flange according to the three different UK resources can be found for normal weight concrete. Slab depth is measured from the face exposed to fire.

For 90 minutes of fire exposure, the temperatures in the top (Table 2) and the bottom (Table 3) fibres of the concrete flange above the steel sheet can be obtained (i.e. X = 130 mm, and X = 60 mm, respectively, according

Conclusions

1. The UK NCCI gives temperature profiles at/above ribs and between ribs for composite slabs; in the paper, a weighted average temperature is suggested to assess the sagging bending resistance of the composite beams design under fire.

2. The temperature distribution profile in the composite slab has generally minimal impact in the composite beam sagging plastic bending resistance because: (i) only the top concrete strips are usually needed to obtain section equilibrium, which are not significantly affected by the slab temperature; (ii) differences in the position of the plastic neutral axis are usually small between the approaches; (iii) as the concrete flange tends to be more resistant at elevated temperature than the steel, even if the slab temperature is actually higher than considered, only small changes in the neutral axis are expected, as a small increase in the assumed slab depth increases considerably the slab resistance.

3. For assessing the resistance of the slab, generally no reduction in strength is needed (ambient temperature may be assumed). An alternative often used, which is to assume the slab temperature is equal to 40% of the steel top flange temperature (a rule used to assess studs resistance under fire), can be seen as a conservative solution.

$M_{pl,rd,fire}$ [kNm]	Slab temperature profile case							
η	1	2	3	4	5	6	7	8
0.00	37.71	37.71	37.71	37.71	37.71	37.71	37.71	37.71
0.25	60.22	60.22	60.22	60.22	60.22	60.22	60.22	60.22
0.50	76.24	76.24	76.24	76.24	76.24	76.24	76.24	76.24
0.75	91.41	91.41	91.41	91.41	91.35	91.30	91.36	91.34
1.00	105.37	105.25	105.25	105.08	105.00	104.95	105.01	104.99

Table 4 – Results for 6 m span beam: UB 203 x 133 x 25; Steel critical temperature: 621°C.

$M_{pl,rd,fire}$ [kNm]	Slab temperature profile case							
η	1	2	3	4	5	6	7	8
0.00	199.13	199.13	199.13	199.13	199.13	199.13	199.13	199.13
0.25	284.60	284.60	284.60	284.60	284.60	284.60	284.60	284.60
0.50	335.08	335.08	335.08	335.08	335.08	335.08	335.08	335.08
0.75	375.67	375.44	375.44	375.10	374.93	374.82	374.95	374.92
1.00	413.06	412.83	412.83	412.49	412.33	412.22	412.34	412.31

Table 5 – Results for 12 m span beam: UB 406 x 178 x 67; Steel critical temperature: 620°C

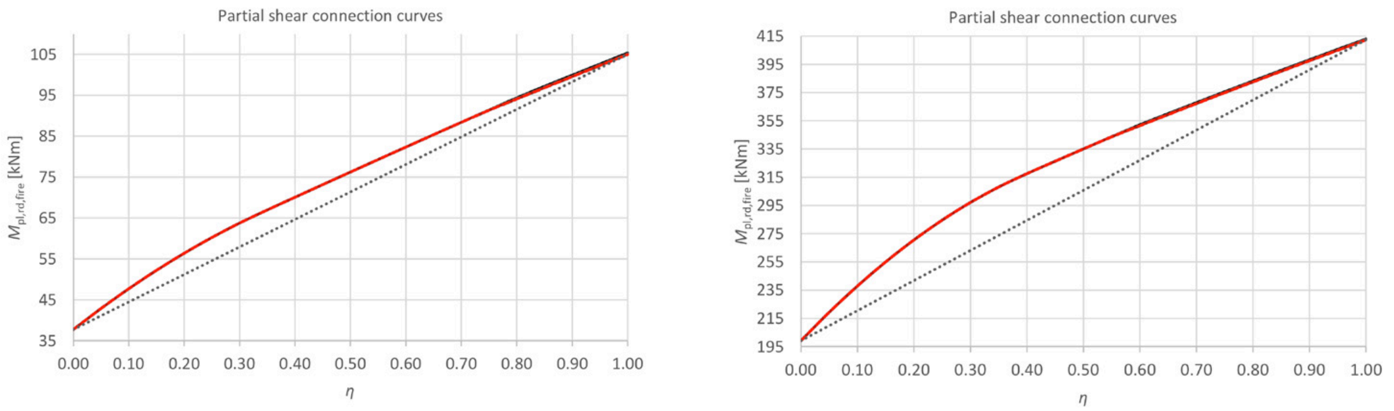

Figure 3 – Partial shear connection curves for the 6 m (left) and 12 m (right) worked examples.

References

1 BS EN 1994-1-2:2005+A1:2014
Eurocode 4 - Design of composite steel and concrete structures - Part 1-2: General rules - Structural fire design
BSI, 2005

2 BS 5950-8:2003
Structural use of steelwork in building - Part 8: Code of practice for fire resistant design
BSI, 2003

3 PN005c-GB
NCCI: Fire resistance design of composite slabs
The Steel Construction Institute

4 NA to BS EN 1994-1-2:2005
UK National Annex to Eurocode 4: Design of composite steel and concrete structures - Part 1-2: General rules - Structural fire design
BSI, 2008;

5 Steel and composite structures: behaviour and design for fire safety
Y. C. Wang, Spoon Press, 2005

6 AS/NZ 2327.1
Composite Structures – Composite steel-concrete construction in buildings
Standards Australia/Standards New Zealand, 2017

Advisory Desk 2018

AD 413
Shear resistances of M12 bolts

Designers using paper or online versions of the Eurocode Blue Book may have noted that the shear resistance of an M12 bolt has different values quoted, depending on the resource selected.

According to BS EN 1090-2, the clearance hole for an M12 bolt is 13 mm. If this diameter hole is used, then the shear resistance may be calculated in the normal way, without any additional factors. This value of shear resistance appears in the online Steel for Life version of the Blue Book.

Clause 3.6.1(5) of BS EN 1993-1-8 allows M12 bolts to be used in 14 mm holes (i.e. slightly oversize), but applying a factor of 0.85 to the quoted resistance. This factor was applied in the paper versions of the Blue Book (P363) and the ArcelorMittal Orange Book resource. It is clearly conservative to apply the 0.85 factor, though the reduction is unnecessary if M12 bolts are used in 13 mm holes.

Contact: **Abdul Malik**
Tel: **01344 636555**
Email: **advisory@steel-sci.com**

AD 414:
Slip-resistant connections to BS EN 1993-1-8

Clause 3.4.1 of BS EN 1993-1-8 describes two types of slip-resistant connections:

- Category B: Slip-resistant at SLS.
- Category C: Slip-resistant at ULS.

Designers often ask when the different categories are appropriate.

Category B is appropriate if slip after SLS but before ULS only produces some unsightly deflections (which may be very unwelcome), but crucially, does not reduce the ultimate resistance of the element or structure. An example might be a splice connection in a roof truss. According to Table 3.2 of the Eurocode, in addition to verifying slip resistance at serviceability the shear and bearing resistance of the bolts must be verified in Category B connections, so that the ultimate resistance of the joint is not reduced even if slippage occurs after SLS.

Category C is appropriate when slip below ULS might reduce the ultimate resistance of the element or structure. An example of this might be a plan bracing restraint system to a compression member – for example in a heavily loaded transfer truss. Slippage within the restraint system might reduce the buckling resistance, so this must be prevented.

Contact: **Abdul Malik**
Tel: **01344 636555**
Email: **advisory@steel-sci.com**

AD 415:
Vertical tying of columns and column splices

For compliance with the tying method of providing robustness, vertical and horizontal ties are required for buildings in Consequence Class 2B.

In the accidental action situation, vertical and horizontal tying is required to redistribute loads through the structure via alternative load paths, away from locally damaged areas. This principle is shown in Figure 1. Vertical ties also help to limit the risk of the upper floor being blown upwards in an explosion.

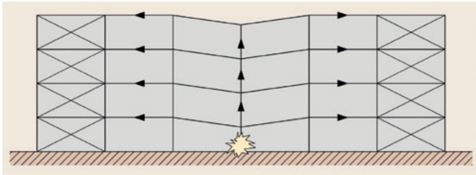

Figure 1

The differences in vertical tying requirements of BS EN 1991-1-7[1] and BS 5950-1[2] has prompted some questions. This AD note reviews those differences and provides recommendations for the design of vertical ties in accordance with BS EN 1991-1-7.

BS EN 1991-1-7, clause A.6 (2) states: "The column should be capable of resisting an accidental design tensile force equal to the largest design vertical permanent and variable load reaction applied to the column from any one storey".

BS 5950-1, clause 2.4.5.3 (c) states: "All column splices should be capable of resisting a tensile force equal to the largest total factored vertical dead and imposed load applied to the column at a single floor level located between that column splice and the next column splice down".

The two differences between the requirements are:

1) The load combination to use for the derivation of the level of loading i.e. accidental or normal ULS load combination.
2) The length of column to be consider to determine the maximum floor load to be considered i.e. the entire column length or the column length between splices.

The rules for vertical tying presented in EN 1991-1-7 (which are non-material specific) are largely based on requirements from BS 8110-1[3] (clauses 3.12.3.7 and 2.4.3.2), requiring continuous vertical ties from the lowest to the highest floor. In BS 8110-1, the design load is generally taken as the permanent actions plus 1/3 of the imposed load, from any one storey, all factored by 1.05.

When considering robustness, which is an accidental limit state, it is logical to use the accidental load combination, as given in BS EN 1990[4]. This guidance supersedes that provided in SCI publication P391 (section 7.3.2)[5] which proposed that the normal ULS loading should be used.

For Eurocode designs, the guidance in BS EN 1991-1-7 should be followed and the entire column length (and any splice) should be capable of carrying the largest accidental design tension resulting from any one storey.

If loads applied at one storey are very large, possibly because (for example) transfer trusses are supported at that level (see figure 9.2 in P391), the accidental force to be accommodated may dominate the selection of the column (and splice connections) at upper levels. If this is the case, it may be more advantageous to consider the support to the transfer trusses to be a key element, and design against its removal.

Contact: **Andrew Way**
Tel: **01344 636555**
Email: **advisory@steel-sci.com**

1 BS EN 1991-1-7:2006+A1:2014 Eurocode 1. Actions on structures. General actions. Accidental actions
2 BS 5950-1:2000 (BSI 2008) Structural use of steelwork in building. Code of practice for design. Rolled and welded sections
3 BS 8110-1:1997 Structural use of concrete. Code of practice for design and construction. Amended by AMD 9882, AMD 13468. Amendment, August 2007; Amendment, November 2005
4 BS EN 1990:2002+A1:2005 Eurocode. Basis of structural design
5 Structural robustness of steel framed buildings (P391). SCI, 2011

AD 416: Artificially reducing the effective width of slab to satisfy shear connection requirements

In composite construction, the effective width of slab to be used in composite beam design, as calculated from BS EN 1994-1-1 (clause 5.4.1.2) and the former BS 5950-3.1+A1, is based on results from experimental and analytical studies. In the past, designers would sometimes use a smaller effective width in their design in an attempt to satisfy the minimum degree of shear connection requirements (BS EN 1994-1-1, 6.6.1.2). This method has been a matter of controversy as it could lead to situations where the actual number of studs provided is not adequate.

The minimum degree of shear connection requirement is a complex problem which is associated with the overall behaviour of the composite beam, and the stiffness and ductility (slip capacity) of the shear connectors. Therefore, due to the various unknowns and nonlinearities present, it is difficult to justify a relaxation to the codified requirements for a minimum degree of shear connection without proper analysis. For example, a number of parameters have been known to have an effect on shear connection demands such as the span, any asymmetry in the steel flange areas, the steel grade, the construction method (propped vs unpropped) and the utilisation of the beam in bending. As one can imagine, simplified methods such as the one in question cannot possibly account for all these in a quantifiable manner.

The most recent guidance in SCI P405 was developed based on the results from tests and extensive numerical analyses that accounted for the effects of the above mentioned parameters. A set of alternative shear connection rules that cover different practical cases is provided to complement the rules in BS EN 1994-1-1.

Contact: **Dr Eleftherios Aggelopoulos**
Tel: **01344 636555**
Email: **advisory@steel-sci.com**

AD 417: Resistance of sections to combined shear and bending

This Advisory Desk note reminds designers that the form of the section has a significant impact on the reduction of bending resistance under high shear.

Clause 6.2.8 of BS EN 1993-1-1:2005 deals with the resistance of cross sections to combined bending and shear and first of all states:

(1) Where the shear force is present allowance should be made for its effect on the moment resistance.

It then goes on to say:

(2) Where the shear force is less than half the plastic shear resistance its effect on the moment resistance may be neglected except where shear buckling reduces the section resistance, see EN 1993-1-5.

(3) Otherwise the reduced moment resistance should be taken as the design resistance of the cross-section, calculated using a reduced yield strength … for the shear area.

The reduced yield strength depends on the ratio of design shear force to the shear resistance of the section.

For an I section, the shear area approximates to the area of the web and the flanges still provide their full resistance moment so the reduction in bending resistance may not be more than about 20% when the design shear force equals the shear resistance. For a rectangular section, the full section forms the shear area so the bending resistance reduces to zero under the same circumstances. A Tee section would also behave in a similar way.

Contact: **Dr Richard Henderson**
Tel: **01344 636555**
Email: **advisory@steel-sci.com**

AD 418: Web-post buckling in composite beams with rectangular and elongated web openings

The design of composite beams with large web openings is presented in SCI P355, which has been adopted in the development of software for the design of both hot rolled and fabricated steel sections with openings of various shapes and sizes. In P355, the method for addressing web buckling next to or between rectangular or elongated openings identifies two cases; closely spaced and widely spaced openings. For rectangular openings, the transition between the two cases is taken at an edge-to-edge spacing s_o, equal to the length of the opening ℓ_o. For elongated openings, this transition occurs at an equivalent opening length, which may be taken as $\ell_o - 0.55h_o$.

For widely spaced openings, web buckling next to an opening is checked by considering the local transfer of the vertical shear force in the Tees acting on a strut of width equal to half the opening depth.

For closely spaced openings, the relevant compression force acting on the equivalent strut is taken as equal to the horizontal shear force in the web-post and the check for web-post buckling is based on an inclined strut whose slenderness depends on the spacing of the openings.

The issue in the design of beams with large web openings is the potentially high 'step' in the shear resistance at the transition between closely and widely spaced openings, which occurs due to the high slenderness of the inclined strut. To partly reduce this issue, some changes in the application of P355 are now appropriate, which relax the current rules for long openings. These relaxations align with the current work to provide normative clauses on the design of beams with large web openings in Eurocodes 3 and 4.

Web-post buckling in P355

In P355, the buckling length of the web-post for closely spaced openings is given by:

$\ell_w = 0.7(h_o^2 + s_o^2)^{0.5}$ for rectangular openings (1)

$\ell_w = 0.5(h_o^2 + s_o^2)^{0.5}$ for circular or elongated openings (2)

where:

h_o is the opening height

s_o is the edge-to-edge distance between the openings.

For rectangular and elongated openings, the maximum opening length is $\ell_o \leq 2.5\, h_o$ for unstiffened openings and the minimum edge-to-edge spacing, s_o should exceed $0.5\,\ell_o$. In comparison, for circular openings, $s_o \geq 0.1h_o$ for steel beams and $\geq 0.3h_o$ for composite beams.

Relaxation for adjacent rectangular openings

For adjacent rectangular openings, it is now accepted that to align with the work on large web openings in the new part of Eurocode 3, EN 1993-1-13, the maximum buckling length for web-post buckling between rectangular openings of the same height may be taken as:

$$\ell_w \leq h_o \tag{3}$$

This leads to an upper bound nondimensional slenderness of the web-post given by:

$$\bar{\lambda}_{wp} \leq \frac{3.5h_o}{t_w\lambda_1} \tag{4}$$

where:

$$\lambda_1 = \pi(E/f_y)^{0.5}$$

$\bar{\lambda}_{wp}$ is used to obtain χ_{wp}, which is the reduction factor due to buckling of the web-post acting as a strut. For rolled sections, buckling curve 'a' in EN 1993-1-1 may be used and for fabricated sections, buckling curve 'c' should be used. The buckling resistance of the web-post is given by:

$$N_{wp,Rd} = \chi_{wp}\, t_{w,min}\, s_o\, f_y/\gamma_{M1} \tag{5}$$

where:

$t_{w,min}$ is the smaller web thickness above/below the opening

f_y is the yield strength of the steel

This buckling resistance is compared to the horizontal shear force, $V_{wp,Ed}$, acting in the web-post. The upper bound shear resistance is given by $\chi_{wp} = 1/\sqrt{3} = 0.577$, which corresponds to pure shear resistance of the web-post rather than buckling.

For rectangular openings, a further check should be made on the in-plane moment acting at the top or bottom of the web-post due to the effects of horizontal shear, which may control for narrow web-posts. For a symmetric section, this moment is given by $0.5V_{wp,Ed}\, h_o$, which should not exceed the in-plane bending resistance of the web-post, which is taken as $t_{w,min}\, s_o^{\,2} f_y /(6\gamma_{M1})$.

Relaxation for adjacent elongated openings or circular and elongated openings

The maximum buckling length for web-post buckling between circular or circular and elongated openings of the same height may be taken as:

$\ell_w \le 0.7h_o$

This leads to an upper bound nondimensional slenderness of the web-post given by:

$$\bar{\lambda}_{wp} \le \frac{2.4h_o}{t_w \lambda_1} \qquad (6)$$

Relaxation for adjacent circular and rectangular openings

For adjacent circular and rectangular openings, or openings of different lengths, it is proposed that the transition between closely spaced and widely spaced openings is taken as the average of the two opening lengths. For adjacent circular and rectangular openings, this corresponds to a transition at an edge-to-edge spacing of $s_o = 0.5(\ell_o + h_o)$. It is proposed that the minimum edge-to-edge spacing is $0.25(\ell_o + h_o)$ for the case of adjacent rectangular and circular openings. The upper bound nondimensional slenderness of the web-post is taken as the average of the two openings.

Contact: **Prof Mark Lawson**
Tel: **01344 636555**
Email: **advisory@steel-sci.com**

AD 419: Composite beams with different positions of web openings

SCI publication P355 is widely used to design beams with large web openings. It is adopted in the development of software to design hot rolled and fabricated steel sections with openings of various shapes and sizes.

The purpose of this Advisory Desk note is to address some common practical problems related to adjacent openings of different heights and positions.

1. Unequal adjacent opening heights

In P355 and in the AD 418, the buckling length of the web post for buckling between closely spaced openings on the same horizontal axis is given by:

$\ell_w = 0.7(h_o^{\,2} + s_o^{\,2})^{0.5} \le h_o$ for rectangular openings (1)

$\ell_w = 0.5(h_o^{\,2} + s_o^{\,2})^{0.5} \le 0.7h_o$ for circular or elongated openings (2)

where:

h_o is the opening height (or average height, as defined below)

s_o is the edge-to-edge distance between the openings

For unequal adjacent opening heights, it is proposed that the average height of the openings, $h_{o,eff}$, may be used to determine the slenderness for web post buckling with a lower limit of 0.75 of the larger opening height. This corresponds to the smaller opening height being taken as not less than half the larger opening height. Therefore, the effective opening height, $h_{o,eff}$ replaces h_o in the above equations and is taken as:

$$h_{o,eff} = 0.5\,(h_{o,1} + h_{o,2}) \ge 0.75\, h_{o,1} \qquad (3)$$

where:

$h_{o,1}$ is the height of the larger opening

$h_{o,2}$ is the height of the smaller opening

2. Different eccentricities of adjacent openings

The eccentricity of the opening, e_o, is defined as positive when the centre line of the opening is above the centre line of the beam and negative when it is below. For the checks on web-post buckling, the effective opening height in the above equations for web-post buckling should include the worst case of the difference in eccentricities, which is as follows:

$$h_{o,eff} = 0.5\,(h_{o,1} + h_{o,2}) + |\, e_{o,1} - e_{o,2} \,| \ge 0.75\, h_{o,1} + |\, e_{o,1} - e_{o,2} \,| \qquad (4)$$

where:

$|\, e_{o,1} - e_{o,2} \,|$ is taken as its absolute value, in which $e_{o,1}$ and e_{o2} can have different signs depending on the position of adjacent openings relative to the centre line of the beam and the heights of the adjacent openings are defined as above.

The use of the absolute value of $|\, e_{o,1} - e_{o,2} \,|$ is the worst case for checking web-post buckling. A more precise treatment that takes account of the buckling length is given below.

3. More precise treatment of eccentricities or unequal adjacent opening heights

For unequal adjacent opening heights and positions, the buckling length should be calculated from the dimension, ℓ which is the diagonal distance from the low edge of the opening in the High Shear Side (HSS) to the high edge of the opening at the Low Shear Side (LSS). Various cases are shown in Figure 1. The buckling length for web-post buckling is taken as:

For circular or elongated openings: $\ell_w = 0.5\ell$

For rectangular openings: $\ell_w = 0.7\ell$

For adjacent circular and rectangular openings: $\ell_w = 0.6\ell$

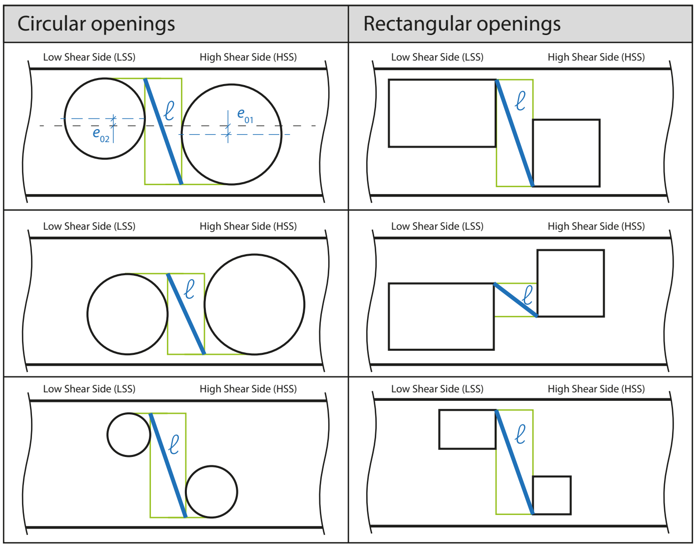

Figure 1:
Treatment of the diagonal distance for web-post buckling between adjacent openings

The dimension ℓ should be calculated by taking $h_{o,2} \ge 0.5h_{o,1}$ to be consistent with the limit in equation (4).

For adjacent rectangular openings, it is also necessary to check the in plane bending resistance of the web-post due to the horizontal force acting at the mid height of the beam. The position of the critical section will depend on the relative position of the openings in the beam depth. For simplicity, the in plane moment in the case of symmetric steel sections is determined from:

$$M_{wp,Ed} = 0.5\,(0.5(h_{o,1} + h_{o,2}) + e_{o,1} + e_{o,2}\,)\, V_{wp,Ed}$$

where:

$V_{wp,Ed}$ is the horizontal shear force acting at the mid height of the beam

This moment should not exceed the elastic bending resistance of the web post which is given by:

$$M_{wp,Ed} = t_w\, s_o^{\,2} f_y /(6\gamma_{M0})$$

where:

s_o is the edge to edge spacing of the openings
t_w is the web thickness
f_y is the yield strength of the steel

Contact: **Prof Mark Lawson**
Tel: **01344 636555**
Email: **advisory@steel-sci.com**

AD 420: Minimum values of shear and bending moment in beams with web openings

Table 3.1 of SCI publication P355 gives minimum values of co-existent shear and bending moment to be used at beam openings. This AD provides clarity on how these minimum values are to be used.

The concern behind the minimum values was to allow for non-uniform loading, to guard against the situation when the shear force at an opening could theoretically be zero. Table 3.1 therefore includes minimum values of the shear force to be allowed for in design. The minimum values of shear force in Table 3.1 have an associated bending moment.

The intention was that the minimum shear force and associated bending moment from Table 3.1 should only be applied if the theoretical shear at an opening was less than the minimum quoted. There is no requirement to apply the minimum bending moment at all openings – the minimum bending moment should only be applied if the minimum shear force is used in design.

Contact: **Prof Mark Lawson**
Tel: **01344 636555**
Email: **advisory@steel-sci.com**

AD 421: Design responsibility for welds in fabricated plate girders

In recent months the SCI has received a number of questions about responsibility for the design of the welds between the web and flanges of a plate girder. These longitudinal welds are an integral part of the member design – and should therefore be sized by the engineer responsible for the design of the beam.

Contact: **Richard Henderson**
Tel: **01344 636555**
Email: **advisory@steel-sci.com**

AD 422: Punching shear check for fin plates in P358

This AD note relates to Check 10 for fin plates in P358 *Simple Joints to Eurocode 3* (the Eurocode "Green Book" on simple connections). Check 10 includes two checks for punching shear (conservative and rigorous), but the value of γ_{M2} is not specified in the text. Confusion is possible because γ_{M2} appears in both BS EN 1993-1-1 and BS EN 1993-1-8, but with different values (1.1 and 1.25 respectively, as given in the relevant UK National Annex).

Since the check does not concern the bolts or welds, but does concern the ultimate material strengths of the fin plate and supporting member, the value of γ_{M2} should be taken as 1.1 from the UK NA to BS EN 1993-1-1.

Contact: **Richard Henderson**
Tel: **01344 636555**
Email: **advisory@steel-sci.com**

AD 423: Reduction in bending resistance due to high shear

When considering the resistance of cross sections under combined bending and high shear, (where the shear is equal to or exceeds half the plastic shear resistance), the resistance moment of the section should be reduced: see BS EN 1993-1-1 cl. 6.2.8(3). A reduced yield strength $(1-\rho)f_y$ where

$$\rho = \left(\frac{2V_{Ed}}{V_{pl,Rd}} - 1\right)^2$$

should be used to calculate the contribution of the shear area to the resistance moment of the section. For an I section, the shear resistance is mainly provided by the web. In cl. 6.2.8(5) the alternative approach calculates the bending resistance by deducting ρ times the plastic modulus of the web from the full plastic modulus of the section, equivalent to using a reduced web thickness.

Similarly, a reduced yield strength $(1-\rho)f_y$ applied to the shear area should be used when considering combined bending, shear and axial force, when the design shear exceeds half the plastic shear resistance of the section.

A reduced plate thickness for the relevant part of the cross section may be used as an alternative. Clause 6.2.10(3) of BS EN 1993-1-1 refers.

Contact: **Richard Henderson**
Tel: **01344 636555**
Email: **advisory@steelconstruction.org**

AD 424: Shear stud length

SCI has been advised that shear studs which are shorter than usual have been placed on the market in the UK, and this AD warns against using them unless the length has been reflected in the design, and unless the studs meet the necessary material specification.

AD 380 indicates that a stud that starts with a manufactured length of 105 mm would typically have a length after welding (LAW) of 100 mm when welded directly to a beam flange and 95 mm when welded through decking. The studs are identified as nominally 100 mm studs. AD 380 also indicates that studs of diameter d = 19 mm and a nominal length of 100 mm may be deemed to satisfy the requirement that a stud extends at least 2d above the height of the decking, when that height is 60 mm. UK practice in composite construction for buildings generally involves the use of through deck welded shear studs. Tests have shown that through deck welded studs of 100 mm nominal length, with 60 mm decking, perform satisfactorily.

A complication is that studs identified as nominally 100 mm long have actual lengths "out of the box" which differ from manufacturer to manufacturer. It is understood that the shorter studs referred to in the opening paragraph are 90 mm before welding, so are likely to be less than 85 mm LAW when welded through decking. Clearly they should not simply be substituted for nominal 100 mm studs unless the design is verified with the shorter length.

All shear studs should conform to EN ISO 13918, as noted in the National Structural Steelwork Specification (NSSS). Composite beam design generally assumes a certain level of slip between the steel and concrete so the studs must be ductile, regardless of the fact that failure is normally in the concrete (at least for the grades of materials typically found in buildings). Annex B of BS EN 1994-1 describes the stud test arrangement to demonstrate ductility.

Contact: **Eleftherios Aggelopoulos**
Tel: **01344 636555**
Email: **advisory@steel-sci.com**

SIGN UP FOR YOUR **FREE SUBSCRIPTION** TO **NSC MAGAZINE**

NSC magazine is available free of charge in a paper format for the UK and Ireland as well as in a digital format for use on tablets, smartphones and desktop computers.

A regularly updated website also carries news of steel construction issues and projects, as well as the NSC digital library containing the current issue and archives.

To register for your copy, email your details to *info@steelconstruction.org*